ABSTRACT

MCCARTHY, KEVIN JOSEPH. Spatial Variability of Belowground Carbon Dynamics Due to Harvested Canopy Gaps in a Southern Appalachian Mixed Oak Forest. (Under the direction of Dr. Jodi Forrester).

Belowground carbon (C) pools in forest ecosystems are highly dynamic systems influenced by a myriad of above- and belowground factors. Carbon assimilated though photosynthesis enters the belowground C pool when allocated to root growth or rhizosphere maintenance or via leaf and litter senescence. It is then stored as root biomass or soil organic matter or lost as carbon dioxide (CO_2) when respired by roots or soil microbial heterotrophs. Carbon assimilation, allocation, and respiration are all heavily regulated by ecological and microclimate conditions and have been shown to respond in inconsistent ways to canopy disturbance. Mature temperate hardwood forests in particular show highly variable site-specific interactions between components of the belowground C pool. This study sought to quantify the effects of harvested canopy gaps on the belowground C dynamics of a Southern Appalachian mixed-oak forest. The objectives were to 1) partition soil respiration into its heterotrophic and autotrophic components and quantify microscale variability along a gap-forest transect and 2) estimate yearly total belowground C allocation (TBCA) in gaps, the unharvested forest surrounding them, and undisturbed control plots using measurements from the other components of the belowground C budget. No consistent difference were found in soil respiration or its partitions between harvested and unharvested locations despite a linear increase in temperature with proximity to the gaps. Average TBCA was more than twice as high in gaps (756.25 $gCm^{-2}yr^{-1}$) and transition zones (844.29 $gCm^{-2}yr^{-1}$) than in control plots (351.25 $gCm^{-2}yr^{-1}$), largely resulting from reduced litterfall and a smaller change in fine root biomass C in gaps. Consistent with other mature temperate hardwood forests, the regression between annual litterfall and soil

respiration in this study was not significant ($r^2 = 0.004$, $P > 0.6$). Southern Appalachian mixed-oak forests are known to be heterogeneous systems, but the high microscale variability demonstrated in this study indicates that more complex models are required when accounting for C budget responses to disturbance than would be necessary in other forest biomes.

Spatial Variability of Belowground Carbon Dynamics Due to Harvested Canopy Gaps in a Southern Appalachian Mixed Oak Forest

by
Kevin Joseph McCarthy

A thesis submitted to the Graduate Faculty of
North Carolina State University
in partial fulfillment of the
requirements for the degree of
Master of Science

Forestry & Environmental Resources

Raleigh, North Carolina

2023

APPROVED BY:

Dr. Jodi Forrester Committee Chair	Dr. Leah Rathbun
Dr. Tara Keyser	Dr. Christopher Maier

BIOGRAPHY

Kevin Joseph McCarthy was born June 13, 1996 in Orlando, Florida. He developed a love for science in his 9th grade biology class and went on to major in Biology at the University of Central Florida. While attending UCF, he spent three years as an undergraduate research assistant in the Aquatic Biogeochemistry Laboratory studying carbon and nitrogen dynamics in wetland ecosystems. After graduating, he was offered a position as a long-term substitute teacher at his alma mater – teaching biology in the same classroom his passion for the subject first developed. His experiences as a teacher bolstered his resolve to further his own education, and this pursuit led him to the Forrester Lab at NC State where he could apply and expand his understanding of carbon dynamics to the southern Appalachian forests.

ACKNOWLEDGEMENTS

I am ineffably grateful to my advisor Dr. Jodi Forrester for her support and mentorship these past two years. Her guidance through the many challenges and setbacks this project brought was instrumental to its success and gave me the opportunity to learn and grow from each one. I would also like to thank my wonderful committee members for the advice and support they gave along the way: Dr. Chris Maier for creating the framework for this carbon study and providing his physiology expertise whenever we needed it; Dr. Tara Keyser for pulling off the immense job of keeping everything at Bent Creek running smoothly so that our field work could be successful; and Dr. Leah Rathbun for boosting my understanding of statistics and providing an invaluable fresh perspective on my thesis.

I cannot begin to express my gratitude to everybody who helped with the field work and lab components of this project. To Philip Whiting and Brandy Benz at Bent Creek Experimental Forest, who always got me out of a pinch when I needed last-minute field help or access to old Bertha if all the department trucks were in use. To Karen Sarsony and Shelly Hooke at the Forest Service Southern Research Station for providing me with the training, materials, and bench space needed for the fractionation portion of my project. To the many undergraduate assistants and the countless hours they spent processing samples, but especially to Amber Payne and Henry Kelso for helping me tackle the grueling summer field work. To everyone in the Forrester lab for the advice, feedback, and games that helped keep me pushing forward. And finally to Morgan Arteman, the best peer mentor I could have asked for.

Funding for this project came from McIntire-Stennis and USDA NIFA award #2019-67019-29463. This research was supported by the intramural research program of the U.S. Department of Agriculture, National Institute of Food and Agriculture, McIntire-Stennis, grant

number NI21MSCFRXXXG043. These findings and conclusions have not been formally disseminated by the U. S. Department of Agriculture and Should not be construed to represent any agency determination or policy.

TABLE OF CONTENTS

LIST OF TABLES

LIST OF FIGURES

Chapter 1: Total belowground carbon allocation changes with canopy gap harvest in a Southern Appalachian mixed-oak forest

Introduction

Belowground carbon (C) pools represent a continuum of organic matter from living roots to freshly senesced litter, across decomposition gradients to more recalcitrant mineral soil fractions (Clifton-Brown et al. 2007). In forest systems, loss of C from soil and root respiration are typically offset by C inputs from litter and belowground C allocation, assuming no major changes in C storage (Raich and Nadelhoffer 1989). Plants allocate anywhere from 20-70% of gross primary production (GPP) belowground for the production and maintenance of roots and mycorrhizal fungi (Keyes and Grier 1981; Gower et al. 1996; Ryan et al. 1997; Giardina et al. 2003; Harmon et al. 2004; Field and Kaduk 2004; Fahey et al. 2005; Litton et al. 2007; Abramoff and Finzi 2016), so small changes in belowground C allocation can greatly alter soil C storage and efflux (Hogberg et al. 2001; Maier et al. 2004). Recent work has demonstrated a strong link between canopy productivity and belowground C flux, indicating that aboveground sink strength controls belowground C allocation (Baldocchi 2008; Vargas et al. 2011). In addition, fine root exudation and turnover and carbon allocated to mycorrhizae are important soil carbon inputs (Kuzyakov 2002; Jones et al. 2009). For example, the formation of new soil carbon is related to rhizosphere carbon flux and respiration, indicating that soil heterotrophic respiration is a key ecosystem process linking GPP, NPP, and net ecosystem production (Raich and Schlesinger 1992; Malhi et al. 1999; Finzi et al. 2015; Li et al. 2021).

Although a simple relationship between soil respiration (R_S) and litterfall is evident for temperate forests at a global scale (Gower et al. 1996), a number of forest types diverge from this pattern, including mature temperate hardwood forests (Davidson et al. 2002). Assumptions made

to simplify this relationship may not be appropriate in disturbed forests where the pools of soil organic matter, roots, and litter are not a steady state, and mature temperate hardwood forests occur across the eastern United States as a result of disturbance and land-use history (Lorimer 1980). Disturbances from pests and pathogens are expanding and becoming even more frequent, although in southeastern forest types harvesting is still a major source of forest disturbance (Cohen et al. 2016). Therefore understanding the response of TBCA following disturbance in a mixed hardwood forest is increasingly important for characterizing future terrestrial carbon cycling.

A component approach to estimating TBCA uses measurements of the belowground C budget to extrapolate the TBCA flux that cannot be directly measured (Raich and Nadelhoffer 1989). Giardina and Ryan (2002) incorporated changes in soil C stores to this approach, increasing its efficacy in disturbed systems and over seasonal or yearly scales. Loss of forest canopy following harvesting or natural disturbance has been shown to affect soil respiration (Kurth et al. 2014; Lewandowski et al. 2019), fine root biomass C and growth (Wilkczynski and Pickett 1993; Bauhus and Bartsch 1996), litterfall (Forrester et al. 2013), and soil C (Jandl et al. 2007), however the magnitude and direction of these changes can vary by ecosystem and in some cases are highly site-specific. A study done by Nave et al. (2011) found a reduction in belowground C allocation in trees having undergone stem girdling treatments, however more research is needed into the effects of photosynthate disruption on belowground processes on larger ecosystem scales (Savage et al. 2016). Applying the component approach to direct measurements of these C pools may help elucidate the implications of disturbance to TBCA in mature temperate forests.

The goal of this study was to identify changes in belowground C dynamics in response to disturbance in a Southern Appalachian mixed oak forest. We used a component approach (Giardina and Ryan 2002) to estimate the effects of harvest on forest C budget in a second growth mixed oak forest and whether the size of canopy gaps influenced the degree of change. In a replicated field experiment, we quantified the litterfall inputs, soil CO_2 efflux, fine root production, and the active, slow, and passive cycling soil C pools as a function of gap size and proximity to canopy gaps to understand the mechanisms controlling TBCA. We hypothesized a reduction in TBCA associated with harvested gaps and increase in C loss through soil CO_2 respiration (Scharenbroch and Bockheim 2008; Nave et al. 2011), with these changes being more prevalent in larger gaps. Testing these responses will help us better understand the C budget implications of disturbance regimes in Southern Appalachian mature temperate forests.

Methods

Site Description

This study is part of a large-scale experiment established in 2019 to test an expanding-gap silvicultural approach (known as "femelschlag") in managing for increased oak and hickory success in the Southern Appalachian mixed oak forests. The study site is located at the Southern Appalachian Femelschlag Experiment (SAFE) located in the Pisgah National Forest, North Carolina (35°28'N, 82°40'W). The site is a mature mixed oak forest dominated primarily by oaks (*Quercus spp.*), hickories (*Carya spp.*), poplar (*Liriodendron tulipifera*), and red maple (*Acer rubrum*) (Grover et al. 2023). Soils are deep, stony, well-drained inceptisols and ultisols of the Edneyville, Chestnut, Toecane, and Tusquitee series. Average monthly temperatures range from -3.2 to 7.9°C in January and 16.5 to 28.0°C in July, and the 30-year mean annual

precipitation is 1480 mm (https://www.ncei.noaa.gov/access/monitoring/climate-at-a-glance/divisional/time-series).

Soil Respiration

The replicated silvicultural manipulation was established across six stands (approximately 61 ha area). Following pre-treatment vegetation inventories, initial harvests of 72 gaps testing two gap sizes (small gaps ranging from 0.14 to 0.44 ha; large gaps ranging from 0.70 to 1.30 ha) occurred in January 2019. A subset of twelve harvested treatment plots and three undisturbed control plots were selected for belowground C measurements. Along the north transect of each gap, five PVC (polyvinyl chloride) soil collars (20 cm diameter x 10 cm height) were installed at 7.5 m intervals beginning 15 m into the unharvested forest from gap edge and extending 15 m into the gap. Collars were numbered 1 to 5, with collar 1 being the northmost forest collar and collar 5 being the southmost gap collar. In control plots, three PVC collars spaced 7.5 m apart were installed in a north-south conformation.

Soil CO_2 flux was measured using a LI-COR LI-7810 infrared gas analyzer (LI-COR Biosciences, Lincoln, NE) with 8100-01S Smart Chamber attachment. Respiration was measured on 11 days in 2021 and 8 days in 2022. Simultaneously with CO_2 flux, discrete soil temperature was recorded at 2.5 cm and 7 cm depth using paired thermometers and % soil moisture was recorded using a moisture meter (HH2 Moisture Meter, Delta-T Devices, Cambridge, UK) with soil moisture probe attachment (ML3 ThetaProbe Soil Moisture Sensor, Delta-T Devices, Cambridge, UK). Tri-hourly temperature was recorded using iButton temperature loggers (Maxim Integrated Products Inc., Sunnyvale, CA) buried approximately 5 mm below the soil surface within 10 cm of each collar. Daily average soil respiration (R_S) was estimated using daily average temperature from the iButtons with models developed between instantaneous CO_2 flux

and discrete temperature at each collar location. Over half of our collars had an $r^2 > 0.9$, with the average $r^2 = 0.88 \pm 0.01$. Collar-level soil moisture was poorly correlated with R_S (average $r^2 = 0.30 \pm 0.02$) and was not included in the model.

Litterfall

Litterfall was measured seasonally from December 2021 to March 2023. Litter was collected in four 0.18 m^2 traps placed in 7.5 m intervals along the north transect of each plot (three traps in control plots) correlating with soil respiration collars. Following collection, litter was returned to the laboratory and dried at 50°C. Litter samples were sorted by branches (>0.5 cm diameter), twigs (<0.5 cm diameter), leaves, and miscellaneous (all other litter, including fruit, seeds, flowers, et cetera), and sorted litter was redried and weighed. Samples were grouped by categories within each plot for total C analysis.

Fine Roots and Soil Fractionation

Fine root biomass C was estimated from soil cores (5 cm diameter x 15 cm deep) collected at each subplot in December 2021, March, June, September, and December 2022. Samples were stored at 3°C until processed. Soils were passed through a 1 mm sieve and hand-sorted by size (< 1 mm, 1-2 mm, >2 mm) and living verses dead based on texture and visual inspection (ArchMiller and Samuelson 2016). Roots were washed to remove soil, dried at 50°C, and weighed. A subsample from each combination of treatment, subplot, and size class was finely ground and analyzed for total C. Soil from 30 cores sampled in March 2022 was saved for mineral soil C density fractionation. Soils were physically separated into density fractions using lithium heteropolytungstate (LST) solutions at five densities: 1.65 g/mL, 1.85 g/mL, 2.25 g/mL, and 2.50 g/mL. For each density, 30g wet soil was weighed into each of ten 50mL centrifuge tubes. 50mL of LST was added to each tube, and tubes were placed on a shaker table at 155 rpm

for 3 hours. Tubes were then centrifuged at 90 rpm for 30 minutes, and the LST solution and any floating material poured into individual beakers. The solution was filtered (Whatman binder-free glass microfiber filters; GF/F; #1825-070; 7cm) to separate the soil from the LST, and the soil was scraped from the filter into labeled vials to be dried and weighed.

Total Belowground Carbon Allocation

Building on the approach by Giardina and Ryan (2002), TBCA ($gCm^{-2}yr^{-1}$) was calculated as:

$$\sum_{\emptyset}^{t} TBCA = \sum_{\emptyset}^{t} R_s - \sum_{\emptyset}^{t} C_L + \Delta C_R + \Delta C_O + \Delta C_S + err.$$

where Ø and t are the starting and ending time, respectively, R_S is soil respiration ($gCm^{-2}yr^{-1}$), C_L is for litterfall C ($gCm^{-2}yr^{-1}$), C_R is root C ($gCm^{-2}yr^{-1}$), C_O is organic layer C ($gCm^{-2}yr^{-1}$), and C_S is mineral soil C ($gCm^{-2}yr^{-1}$). The err term acknowledges the C flux unaccounted due to the nature of ecological modeling. This model incorporates the mass-balance approach of Raich and Nadelhoffer (1989), assuming the mass of C entering the system is equal to the mass of C leaving the system plus the mass of C stored within the system. In practical terms, C inputs from litterfall and TBCA during a given time period should be equal to C loss through R_S plus any changes to root or soil C during that time period (Figure 1.1). For this study, our time period began December 8, 2021 and ended December 2, 2022. Changes in organic layer and mineral soil C were assumed to be zero (Giardina and Ryan, 2002).

Statistical Analysis

To test the effect of gaps on each component of the belowground C budget, data collected at each collar location was grouped into three zones based on proximity to the gaps. In each treatment plot, collars within the gaps (collars 4 and 5; n = 22) were grouped as the “gap” zone,

collars north of the gap (collars 1, 2, and 3; n = 34) were grouped as the "transition" zone, and the three collars in each control plot (n = 9) were grouped as controls. Due to the lack of independence between gap and transition zones, three T-tests were performed for each C component (TBCA, litterfall, R_S, Δ root biomass, and mineral soil C fractions) to find differences between controls and gaps, controls and transition zones, and gaps and transition zones. To test the effects of gap size for each C component, treatment plots were grouped by gap size and compared with a T-test using the average response from each plot as replicates. Treatment main effects were considered significant at $\alpha = 0.05$. All statistical analyses were performed in R (4.3.1) and JMP Version 16 (SAS Institute Inc., Cary, NC).

Results

Components of TBCA

Belowground C allocation (TBCA) in the gap and transition zones was nearly or more than double that measured in the controls (Table 1.1). Allocation differed significantly between control plots and transition zones (P = 0.0077) and nearly significantly between control plots and gaps (P = 0.0563; Table 1.2). There was a marginally significant difference between large and small gap sizes (P = 0.0906) but no difference between transition zones and gaps (P = 0.3925). TBCA, R_S, and litterfall had higher variability in large plots than in small plots (Table 1.1).

Across all gap sizes and zones, R_S represented the largest flux in the belowground C system (Figure 1.2, Table 1.1). Site-wide annual C loss from R_S averaged 1072.73 $gCm^{-2}yr^{-1}$. While it did not vary significantly between different gap sizes or zones, there was a slight stepwise increase in average yearly R_S between the controls, small gaps, and large gaps (Table 1.2). Monthly R_S followed expected temperature trends, peaking in late-July and dropping off mid-September when temperatures began to decline (Figure 1.3).

Total annual litterfall was significantly higher in the controls (394.15 $gCm^{-2}yr^{-1}$) than in the transition zones (240.24 $gCm^{-2}yr^{-1}$; P = 0.0065) or gaps (270.02 $gCm^{-2}yr^{-1}$; P = 0.0080; Figure 1.2, Table 1.2). Despite the reduced canopy cover of the gaps, there was no significant difference in annual litter input between transition zones and gaps (P = 0.3251) or between large and small gaps (P = 0.8815). The ratio of TBCA to litterfall C in the treatment plots was three times higher in the gaps ($\mu = 3.02 \pm 0.54$; P = 0.0715) and four times higher in the transition zones ($\mu = 4.00 \pm 0.53$; P = 0.0140) than in the control plots ($\mu = 0.90 \pm 0.03$).

Mineral soil C turnover did not differ significantly by zone for any density fraction (Table 1.3). We observed a slight increase in light, high-turnover C densities within gaps, however the differences were not significant at $\alpha < 0.1$.

Fine Roots

The change in root mass accounted for 11.1±0.01%, 13.0±0.02%, and 17.5±0.24% of the total TBCA calculation in gaps, transition zones, and controls, respectively. The direction of this contribution varied greatly by location, with only 60% of collar locations having lower fine root biomass C in Dec 2022 than in Dec 2021 (Figure 1.4).

Fine root biomass C was consistently lower in the gaps than in either transition zones or controls, though this difference was only significant in June (P < 0.001) and Dec 2022 (P < 0.05; Figure 1.4). Likewise, fine root biomass C was generally lower in large gaps than in small gaps, but this effect was only significant in Dec 2021 (P < 0.001). Fine root biomass C varied slightly by season (P < 0.1), with biomass from Dec-Mar being significantly higher than Sept-Dec 2022 (Figure 1.5, Table 1.4). Across all plots, fine root biomass C averaged 478±43, 588±41, 510±56 , 528±29, and 425±26 gCm^{-2} in Dec 2021, Mar, June, Sept, and Dec 2022, respectively. Biomass C of larger fine roots (>2 mm diameter) was generally greater than that of smaller fine roots (< 2

mm diameter) with the exception of Sept which had significantly higher biomass C in roots of the smaller size class. Carbon content of the roots (%C) varied by season, with roots in warmer months generally containing more C than in colder months (Figure 1.5, Table 1.4).

Discussion

Overall, we saw a considerable increase in TBCA in gaps and transition zones compared to the controls. This increase seems to be largely mediated by a reduction in litterfall in the gaps (251±13 $gCm^{-2}yr^{-1}$) compared to the controls (394±28 $1gCm^{-2}yr^{-1}$). The reduction in fine root biomass C in canopy gaps compared to the transition zone is consistent with previous studies in temperate (Wilkczynski and Pickett 1993; Bauhus and Bartsch 1996) and tropical (Denslow et al. 1998; Leuschner et al. 2006) forests. Leuschner et al. (2006) found a negative correlation between percent canopy cover and fine root biomass across 12 plots of varying canopy covers and land use in an Indonesian tropical forest. While differences in biomass were apparent in two seasons in our Southern Appalachian gaps, they were inconsistent across the full year. This may be an artifact of the sequential coring method we used to collect fine roots (Hendricks et al. 1993), however we felt this was the best method given our study location and logistical constraints. Using ingrowth cores sampled quarterly for a year, Bauhus and Bartsch (1996) found beech fine root growth to be consistently higher in stands than at the edge of gaps, and lowest at the gap center.

Assuming that C stocks are at a steady state has been a controversial proposal when measuring belowground C budgets, with studies disagreeing over whether soil organic matter, roots, and litter should be considered constant (Raich and Nadelhoffer 1989) or changing (Gower et al. 1996). Using a simple relationship between R_S and litterfall, Raich and Nadelhoffer (1989) found annual R_S ($gCm^{-2}yr^{-1}$) to be three times higher than annual litterfall ($gCm^{-2}yr^{-1}$) on a global

scale in forest ecosystems. Davidson et al. (2002) found similar results for the global scale, but when using data from only mature temperate hardwood forests found the regression between R_S and litterfall was not significant. The regression between R_S and litterfall in our study was similarly non-significant ($r^2 = 0.004$; Figure 1.6), suggesting additional complexity is required when modeling TBCA in mature temperate hardwood forests. The inclusion of changing root biomass in our TBCA calculations resulted in an average difference in TBCA of 19.2 ± 0.14% compared to if root growth was not accounted for. Root dynamics are highly variable in disturbed forest systems (Wilkczynski and Pickett 1993; Jones et al. 2003; Taskinen et al. 2003), and our data suggests that including them is necessary for a thorough accounting of TBCA.

We observed no significant variability in mineral soil C densities between disturbed and control plots. Low density organic matter is generally more labile and quickly mineralized, leading to high turnover rates, whereas higher density fractions are more recalcitrant and have slow turnover (Hassink 1995; Christensen 2002). The effect of forest harvest on mineral soil C is varied, but an analysis by Nave et al. (2010) of 75 studies conducted in temperate hardwood forests found a 13% and 7% decrease in mineral C storage in Inceptisols and Ultisols, respectively, following harvest. Among 20 northeastern temperate forests, Petrenko and Friedland (2015) found generally higher concentrations of mineral soil C in >100-year-old forests than in harvested stands, but their results were not statistically significant likely due to the high spatial variability of their study area.

Recorded annual R_S at our site was within range of previous studies in the Southern Appalachians. Previous studies report annual R_S ranging from 880 to 1260 $gCm^{-2}yr^{-1}$ (Bolstad and Vose 2005; Oishi et al. 2018). Studies within the same region using different methods to measure R_S have reported CO_2 measurements ranging from 0 to 9.1 $\mu mol\ m^{-2}s^{-1}$ (Bolstad et al.

2004; Vose and Bolstad 2007), the upper end of which is lower than our maximum recorded CO_2 flux of 13.3 μmol $m^{-2}s^{-1}$. R_S is most strongly mediated by soil temperature, though soil moisture and substrate supply have been shown to affect the heterotrophic component of R_S (Davidson et al. 2012; Savage et al. 2018). Due to the strong R_S by temperature fits (r^2 = 0.66 to 0.99 by subplot) and poor correlation between R_S and soil moisture at our site, we did not feel the need to apply a more complex model to our R_S measurements.

We saw no change in R_S between gaps, transition zones, and controls. R_S is comprised of autotrophic and heterotrophic components – respiration from roots and soil microbes, respectively (Kuzyakov 2006). Estimates of the proportional contribution of autotrophic and heterotrophic respiration to total R_S vary considerably by ecosystem and measurement method (Subke 2006). Previous research at the study site found high variability in the ratio of heterotrophic to total soil respiration (McCarthy et al. in prep), however most studies find heterotrophic respiration to contribute about 80% to total soil respiration (Heim et al. 2015; ArchMiller and Samuelson 2016; Savage et al. 2018). Heterotrophic respiration is in part regulated by available soil C substrates so the reduction of litterfall in the gaps may have hindered heterotrophic respiration to some extent, though it is unclear on what time scale this would occur. Likewise, an increase in TBCA would lead to a similar increase in root respiration due to metabolic activity from growth and maintenance. It is unclear from our data whether these directly lead to there being no change in R_S between gaps, transition zones, and control plots, but future research should explore the relative contribution of these C inputs.

Conclusion

In this study, we used a component approach to estimate the influence canopy gaps have on total belowground C allocation (TBCA) by measuring litterfall, soil respiration (R_S), fine

roots, and mineral soil C turnover in harvested canopy gaps, the forest surrounding them (transition zone), and undisturbed control plots. Between Dec 2021 and Dec 2022, TBCA was significantly higher in gaps and transition zones than in the control plots. This is contrary to conventional wisdom suggesting a reduction in TBCA in response to canopy disturbance. Litterfall was higher in the control than the treatment plots but did not differ between the gaps and transition zones. Canopy gaps had no clear effect on R_S or mineral soil C turnover. The nonlinear relationship between litterfall and R_S is consistent with other mature temperature hardwood forests (Davidson et al. 2002), suggesting additional complexity is required for TBCA estimations in this forest type, possibly due to the inherent role disturbance plays in these systems. As further evidence of this, accounting for the change in fine root biomass C resulted in up to a 17.5% difference in our TBCA estimation compared to if we had not included them. Southern Appalachian mixed oak forests are highly complex and heterogenous forest systems. This study underlines the importance of understanding how each component of the belowground C budget responds to aboveground disturbance and how they play into the belowground C dynamic model as a whole.

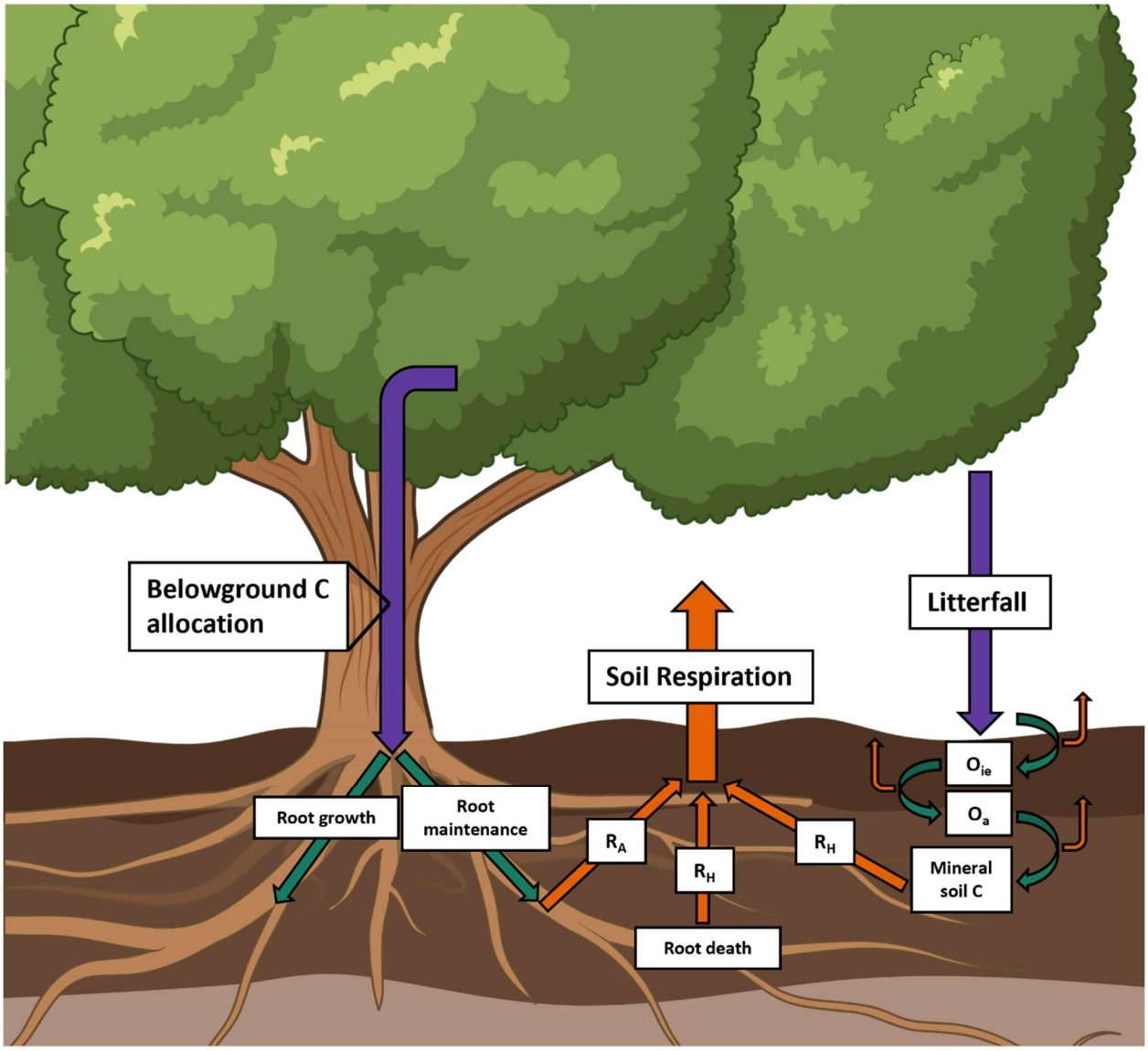

Figure 1.1 The flow of C through the belowground C pool. Inputs (purple arrows) include belowground C allocation, used by roots for growth and maintenance, and litterfall, which decomposes into the organic (O_{ie}, O_a) and mineral soil layers. Root exudates (R_A) and heterotrophic respiration (R_H) represent C loss (orange arrows) from the system as soil respiration. Created with BioRender.com

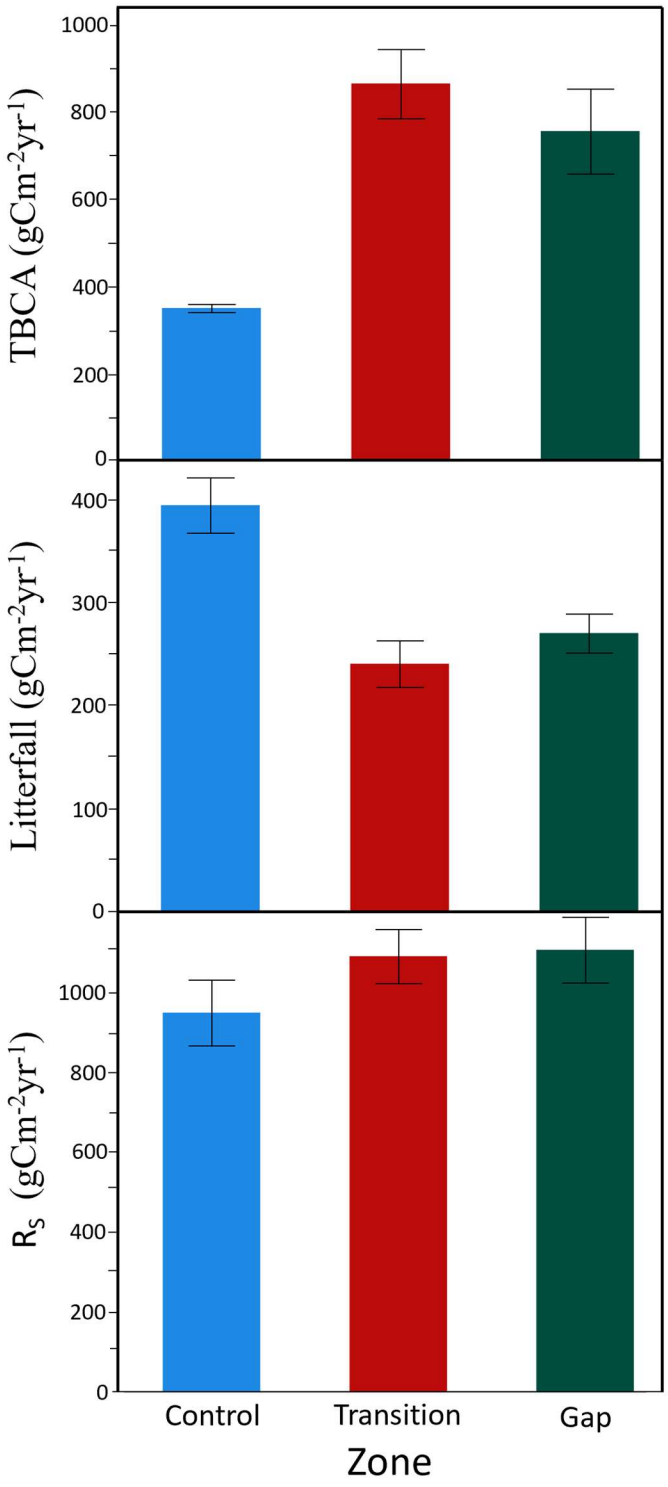

Figure 1.2 Annual average TBCA, Litterfall, and R_S for control, transition, and gap zones in 2022. Units in $gCm^{-2}yr^{-1}$. Error bars indicate one standard error from the mean.

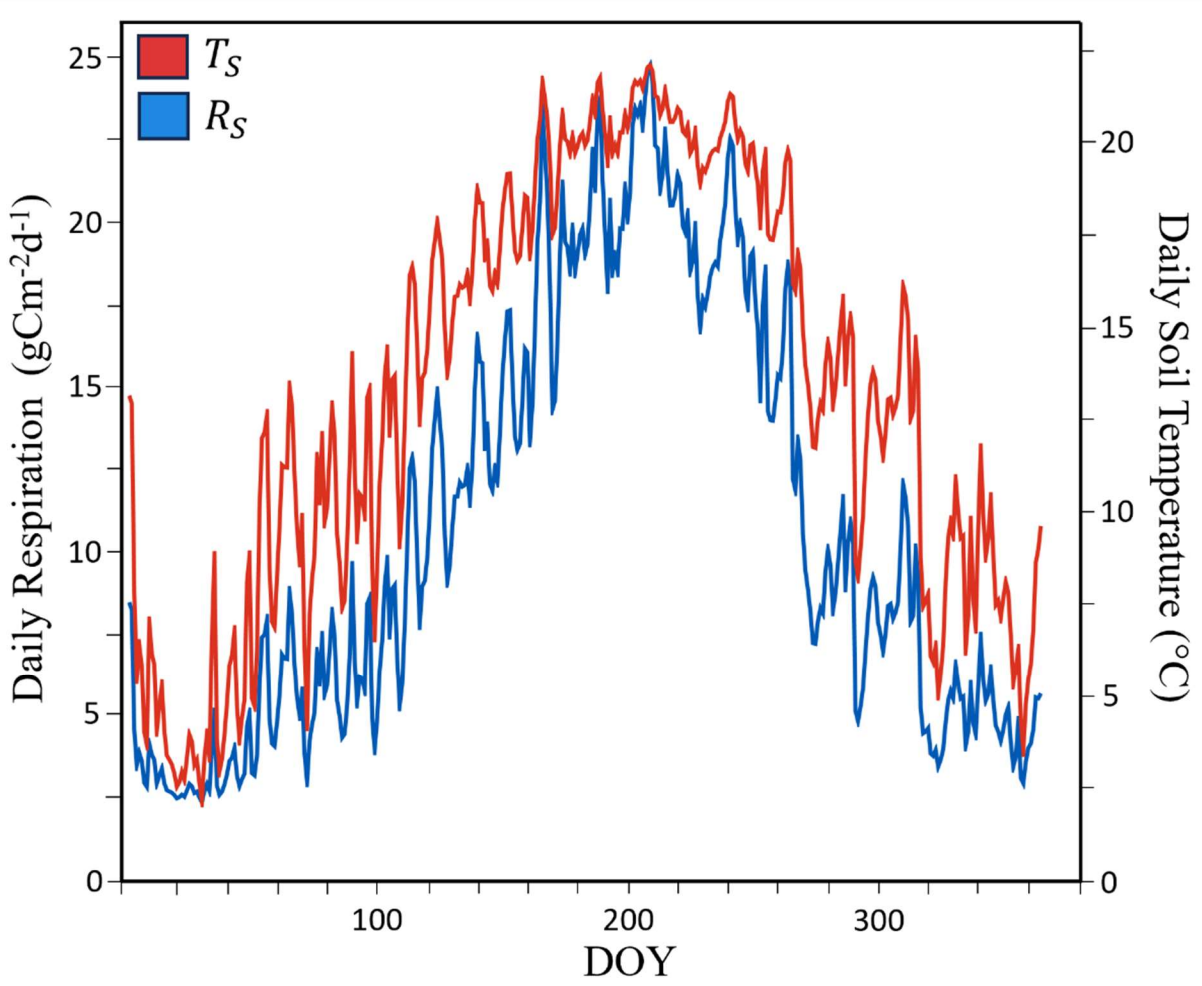

Figure 1.3 Sitewide daily average R_S ($gCm^{-2}d^{-1}$) and T_S (°C) in 2022. Soil temperature indicated by the top red line (values shown on the right Y-axis) and soil respiration indicated by the bottom blue line (values shown on the left Y-axis).

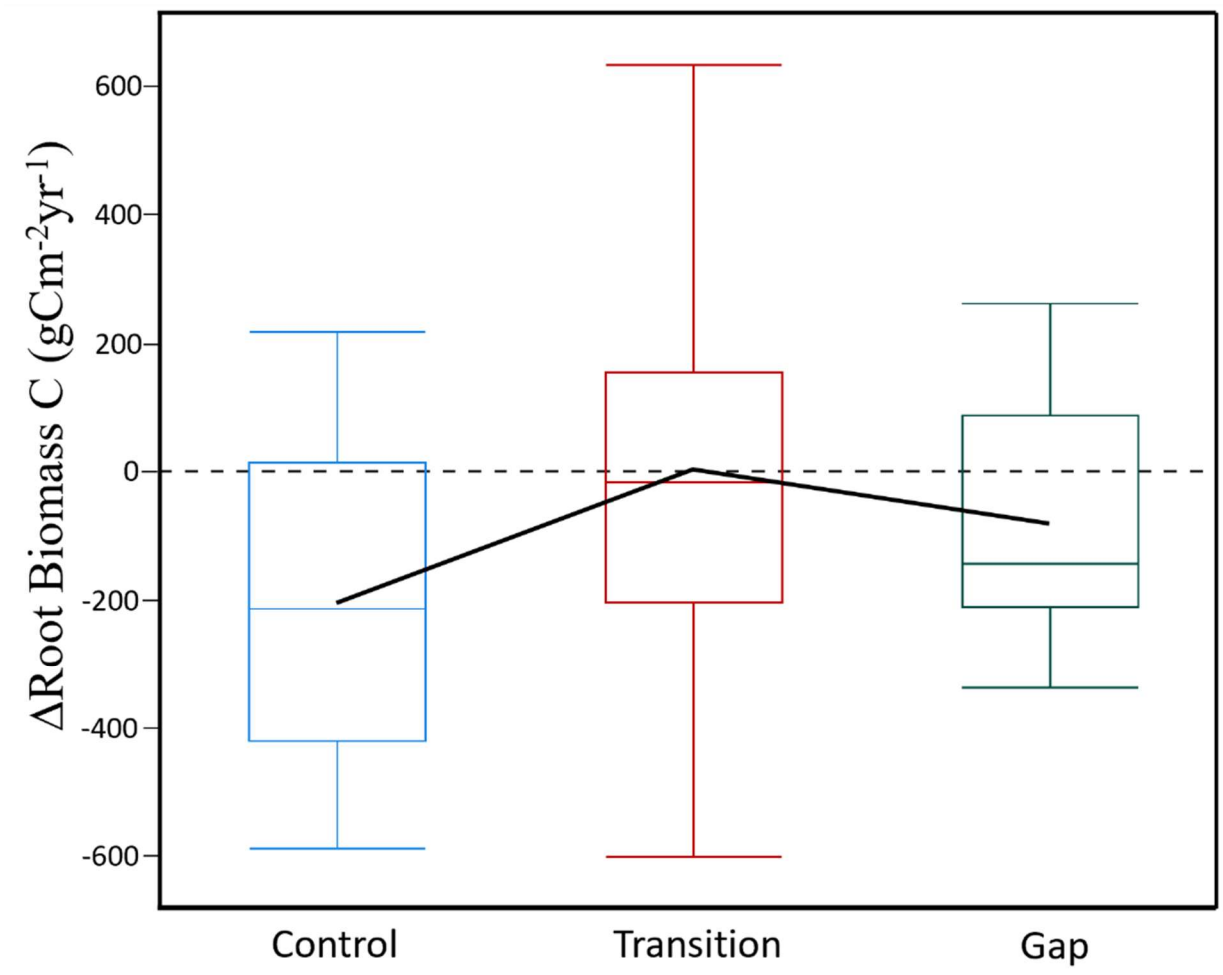

Figure 1.4 Distribution of the change in root biomass C ($gCm^{-2}yr^{-1}$) between December 2021 and December 2022 for collars locations within control, transition, and gap zones. Solid line indicates difference in mean between each zone.

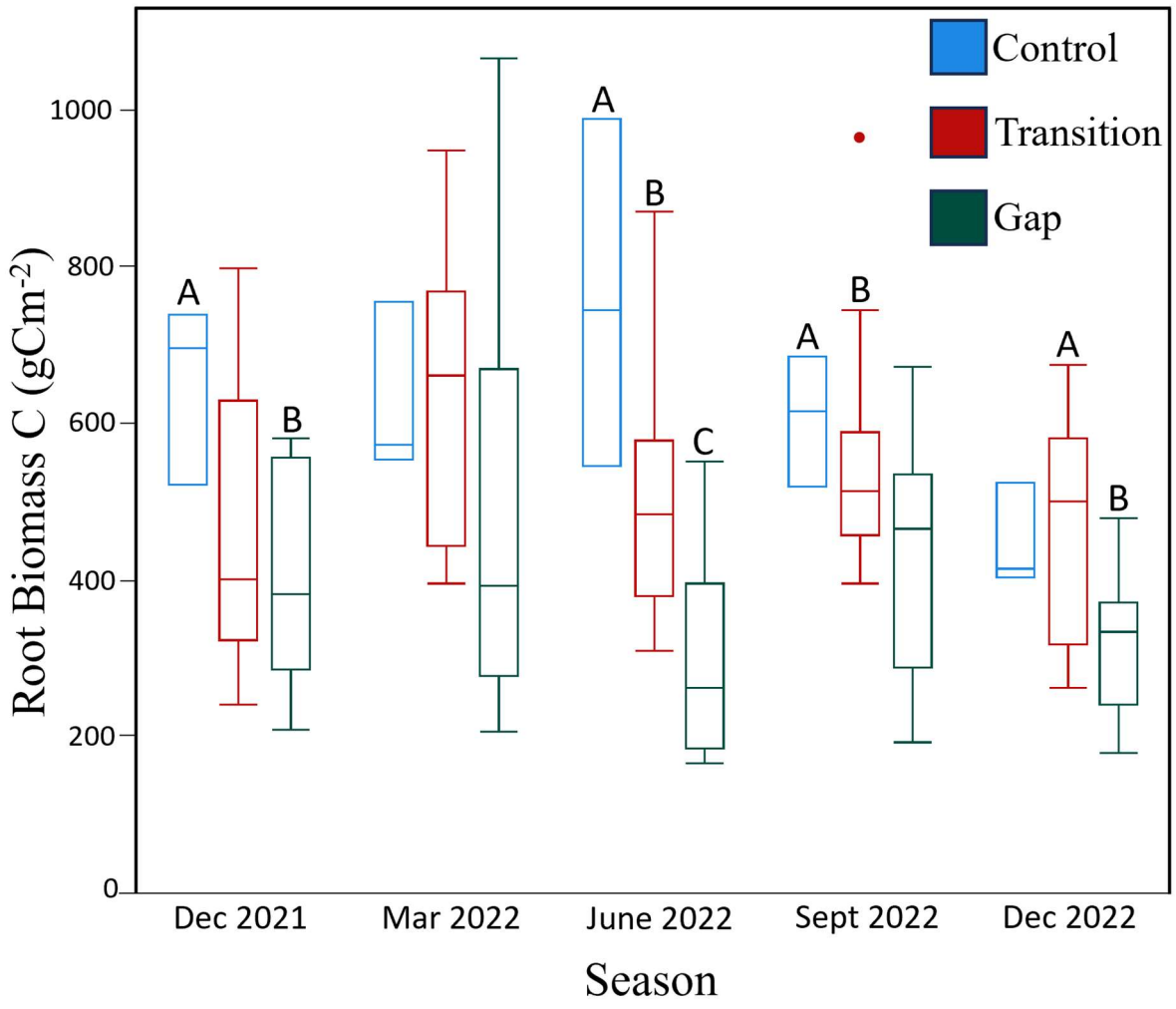

Figure 1.5 Average fine root biomass C (gCm^{-2}) measured within control, transition, and gap zones during each season from Dec 2021 to Dec 2022. Root samples were collected using sequential coring at each collar location and averaged by zone.

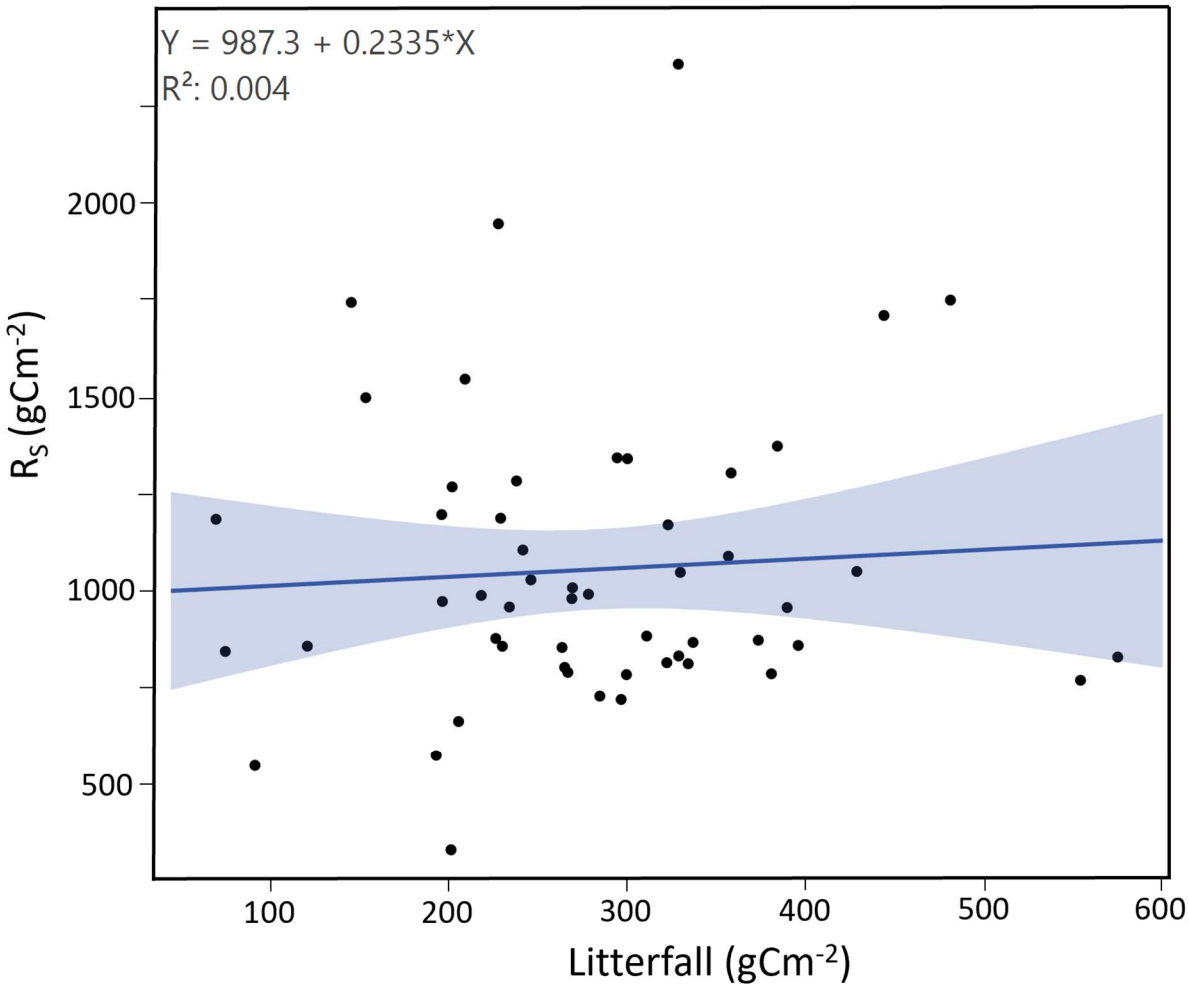

Figure 1.6 Linear regression of annual soil respiration ($gCm^{-2}yr^{-1}$) and annual litterfall ($gCm^{-2}yr^{-1}$) at each measured collar location. The regression is not significant at $\alpha = 0.05$ ($P > 0.05$; $r^2 < 0.01$).

Table 1.1 Mean (SE) contribution ($gCm^{-2}yr^{-1}$) of belowground carbon allocation, litter, soil respiration, and Δ root biomass C to the belowground carbon pool in each gap size and zone.

Gap Size	Zone	C Pool ($gCm^{-2}yr^{-1}$)			
		TBCA	Respiration (R_S)	Litterfall (C_L)	Δ Roots (C_R)
Control	Forest	351.25 (139.46)	950.81 (105.25)	394.15 (28.51)	-205.41 (-3.20)
All Gaps	Transition	844.29 (70.01)	1082.10 (51.97)	240.24 (16.53)	2.42 (46.22)
	Gap	756.25 (107.57)	1108.14 (93.06)	270.02 (21.12)	-81.86 (36.56)
Small	Transition	771.09 (93.80)	1099.26 (68.04)	229.72 (19.02)	-98.53 (65.18)
	Gap	563.23 (84.65)	986.74 (80.34)	277.56 (18.72)	-145.95 (54.48)
Large	Transition	909.43 (102.67)	1066.85 (79.01)	249.58 (26.58)	92.16 (59.12)
	Gap	917.11 (174.47)	1209.30 (154.47)	263.74 (36.26)	-28.46 (45.66)

Table 1.2 Pairwise comparisons between each carbon pool (TBCA, soil respiration, litterfall, and Δ root biomass C) and treatment factor (gap size, zone). All values are given in $gCm^{-2}yr^{-1}$. *P* values obtained from T-tests comparing differences between gap sizes or zones.

		C Pool ($gCm^{-2}yr^{-1}$)			
		TBCA	Respiration (R_S)	Litterfall (C_L)	Δ Roots (C_R)
Gap Size	Small Gaps	691.09 (68.19)	1055.98 (52.18)	248.12 (14.28)	-116.77 (44.73)
	Large Gaps	912.50 (91.25)	1123.83 (77.36)	255.24 (21.20)	43.92 (40.82)
	P value	0.0906	0.4537	0.8815	**0.0277**
Zone	Control	351.25 (139.46)	950.81 (105.25)	394.15 (28.51)	-205.41 (-3.20)
	Transition	844.29 (70.01)	1082.10 (51.97)	240.24 (16.53)	2.42 (46.22)
	Gap	756.25 (107.57)	756.25 (107.57)	1108.14 (93.06)	270.02 (21.12)
T-test *P* values					
Control vs Gap		0.0563	0.3642	**0.0080**	0.0741
Control vs Transition		**0.0077**	0.3440	**0.0065**	0.0616
Gap vs Transition		0.3925	0.8829	0.3251	0.1323

Bold indicates a significant difference at α = 0.05

Table 1.3 Density fractions of soil samples collected from the top 15 cm of the mineral soil layer in March 2022. Values indicate the average % contribution of each density fraction to the total sample.

Zone	1.65 g/mL	1.85 g/mL	2.00 g/mL	2.25 g/mL	2.50 g/mL	>2.50 g/mL
Control (n = 4)	0.8 (0.2)	1.2 (0.7)	0.4 (0.1)	5.6 (0.8)	34.4 (6.7)	57.7 (7.8)
Transition (n = 16)	1.4 (0.4)	0.5 (0.1)	0.6 (0.1)	5.2 (0.8)	43.8 (2.5)	48.4 (2.4)
Gap (n = 10)	2.6 (1.2)	1.1 (0.6)	0.9 (0.2)	6.6 (1.1)	41.9 (5.8)	47.0 (5.6)
T-test *P* values						
Control vs Gap	0.4854	0.7668	0.2739	0.7987	0.2148	0.7124
Control vs Transition	0.4815	0.2172	0.3723	0.9549	0.2967	0.3276
Gap vs Transition	0.5930	0.4975	0.4828	0.7571	0.4217	0.7696

Table 1.4 Pairwise comparisons of size class (< 2 mm and > 2 mm diameter) and season (month sampled) for mean fine root biomass C (gCm^{-2}) and mean C content (% C). *P* values obtained from one-way ANOVAs comparing root size classes within a given month or comparing months within a given size class. Values in parentheses indicate standard error.

Month Sampled	< 2 mm (gCm^{-2})	> 2 mm (gCm^{-2})	*P* value (Size)	< 2mm (%C)	> 2mm (%C)	*P* value (Size)
Dec '21	204.2 (13.7)^{b}	274.3 (32.8)^{ab}	0.0583	–	–	–
Mar '22	191.2 (8.8)^{b}	397.5 (37.9)^{a}	**<0.0001**	31.7 (1.7)^{c}	39.4 (1.2)^{bc}	**0.0220**
June '22	187.5 (10.5)^{b}	322.6 (50.4)^{ab}	**0.0139**	42.3 (1.8)^{ab}	45.3 (0.7)^{ab}	0.1805
Sept '22	626.0 (18.4)^{a}	202.2 (25.1)^{b}	**0.0004**	48.8 (1.3)^{a}	46.2 (0.1)^{a}	0.1120
Dec '22	223.0 (17.9)^{b}	201.6 (22.4)^{b}	0.4612	36.4 (3.0)^{bc}	42.2 (0.7)^{c}	0.1335
P value (Month)	**<0.0001**	**0.0005**		**0.0020**	**0.0009**	

Bold indicates a significant difference at $\alpha = 0.05$
Lower case letters indicate significant differences between months at $\alpha = 0.05$

REFERENCES

Abramoff RZ, Finzi AC. 2016. Seasonality and partitioning of root allocation to rhizosphere soils in a midlatitude forest. Ecosphere 7:e01547.

ArchMiller A, Samuelson L. 2016. Partitioning Longleaf Pine Soil Respiration into Its Heterotrophic and Autotrophic Components through Root Exclusion. Forests 7:39.

Baldocchi D. 2008. 'Breathing' of the terrestrial biosphere: lessons learned from a global network of carbon dioxide flux measurement systems. Aust J Bot 56:1.

Bauhus J, Bartsch N. 1996. Fine-root growth in beech (Fagussylvatica) forest gaps. Can J For Res 26:2153–9.

Bolstad PV, Davis KJ, Martin J, Cook BD, Wang W. 2004. Component and whole-system respiration fluxes in northern deciduous forests. Tree Physiology 24:493–504.

Bolstad PV, Vose JM. Forest and Pasture Carbon Pools and Soil Respiration in the Southern Appalachian Mountains.

Christensen BT. 2001. Physical fractionation of soil and structural and functional complexity in organic matter turnover: Turnover of soil organic matter. European Journal of Soil Science 52:345–53.

Clifton-Brown JC, Breuer J, Jones MB. 2007. Carbon mitigation by the energy crop, *Miscanthus*. Global Change Biology 13:2296–307.

Cohen WB, Yang Z, Stehman SV, Schroeder TA, Bell DM, Masek JG, Huang C, Meigs GW. 2016. Forest disturbance across the conterminous United States from 1985–2012: The emerging dominance of forest decline. Forest Ecology and Management 360:242–52.

Davidson EA, Samanta S, Caramori SS, Savage K. 2012. The Dual Arrhenius and Michaelis–Menten kinetics model for decomposition of soil organic matter at hourly to seasonal time scales. Global Change Biology 18:371–84.

Davidson EA, Savage K, Bolstad P, Clark DA, Curtis PS, Ellsworth DS, Hanson PJ, Law BE, Luo Y, Pregitzer KS, Randolph JC, Zak D. 2002. Belowground carbon allocation in forests estimated from litterfall and IRGA-based soil respiration measurements. Agricultural and Forest Meteorology 113:39–51.

Denslow JS, Ellison AM, Sanford RE. 1998. Treefall gap size effects on above- and below-ground processes in a tropical wet forest. Journal of Ecology 86:597–609.

Fahey TJ, Siccama TG, Driscoll CT, Likens GE, Campbell J, Johnson CE, Battles JJ, Aber JD, Cole JJ, Fisk MC, Groffman PM, Hamburg SP, Holmes RT, Schwarz PA, Yanai RD. 2005. The Biogeochemistry of Carbon at Hubbard Brook. Biogeochemistry 75:109–76.

Field Christopher B, Kaduk J. 2004. The Carbon Balance of an Old-growth Forest: Building Across Approaches. Ecosystems 7. http://link.springer.com/10.1007/s10021-004-0142-7.

Finzi AC, Abramoff RZ, Spiller KS, Brzostek ER, Darby BA, Kramer MA, Phillips RP. 2015. Rhizosphere processes are quantitatively important components of terrestrial carbon and nutrient cycles. Global Change Biology 21:2082–94.

Forrester JA, Mladenoff DJ, Gower ST. 2013. Experimental Manipulation of Forest Structure: Near-Term Effects on Gap and Stand Scale C Dynamics. Ecosystems 16:1455–72.

Giardina CP, Ryan MG. 2002. Total Belowground Carbon Allocation in a Fast-growing Eucalyptus Plantation Estimated Using a Carbon Balance Approach. Ecosystems 5:487–99.

Giardina CP, Ryan MG, Binkley D, Fownes JH. 2003. Primary production and carbon allocation in relation to nutrient supply in a tropical experimental forest. Global Change Biology 9:1438–50.

Gower ST, Pongracic S, Landsberg JJ. 1996. A Global Trend in Belowground Carbon Allocation: Can We Use the Relationship at Smaller Scales? Ecology 77:1750–5.

Grover ZS, Forrester JA, Keyser TL, King JS, Altman J. 2023. Growth response, climate sensitivity and carbon storage vary with wood porosity in a southern Appalachian mixed hardwood forest. Agricultural and Forest Meteorology 332:109358.

Harmon MarkE, Bible K, Ryan Michael G, Shaw David C, Chen H, Klopatek J, Li X. 2004. Production, Respiration, and Overall Carbon Balance in an Old-growth Pseudotsuga-Tsuga Forest Ecosystem. Ecosystems. http://link.springer.com/10.1007/s10021-004-0140-9.

Hassink J. 1995. Decomposition Rate Constants of Size and Density Fractions of Soil Organic Matter. Soil Science Soc of Amer J 59:1631–5.

Heim BC, Seiler JR, Strahm BD. 2015. Root Nonstructural Carbohydrates and Their Relationship with Autotrophic Respiration of Loblolly Pine (*Pinus taeda* L.). Communications in Soil Science and Plant Analysis 46:888–96.

Hendricks JJ, Nadelhoffer KJ, Aber JD. 1993. Assessing the role of fine roots in carbon and nutrient cycling. Trends in Ecology & Evolution 8:174–8.

Högberg P, Nordgren A, Buchmann N, Taylor AFS, Ekblad A, Högberg MN, Nyberg G, Ottosson-Löfvenius M, Read DJ. 2001. Large-scale forest girdling shows that current photosynthesis drives soil respiration. Nature 411:789–92.

Jandl R, Lindner M, Vesterdal L, Bauwens B, Baritz R, Hagedorn F, Johnson DW, Minkkinen K, Byrne KA. 2007. How strongly can forest management influence soil carbon sequestration? Geoderma 137:253–68.

Jones DL, Nguyen C, Finlay RD. 2009. Carbon flow in the rhizosphere: carbon trading at the soil–root interface. Plant Soil 321:5–33.

Jones R, Mitchell R, Stevens G, Pecot S. 2003. Controls of fine root dynamics across a gradient of gap sizes in a pine woodland. Oecologia 134:132–43.

Keyes MR, Grier CC. 1981. Above- and below-ground net production in 40-year-old Douglas-fir stands on low and high productivity sites. Can J For Res 11:599–605.

Klingenberg E, Leuschner C. 2018. A belowground perspective of temperate old-growth forests: Fine root system structure in beech primeval and production forests. Forest Ecology and Management 425:68–74.

Kuzyakov Y. 2002. Review: Factors affecting rhizosphere priming effects. Z Pflanzenernähr Bodenk 165:382–96.

Kuzyakov Y. 2006. Sources of CO2 efflux from soil and review of partitioning methods. Soil Biology and Biochemistry 38:425–48.

Leuschner C, Wiens M, Harteveld M, Hertel D, Tjitrosemito S. 2006. Patterns of Fine Root Mass and Distribution along a Disturbance Gradient in a Tropical Montane Forest, Central Sulawesi (Indonesia). Plant Soil 283:163–74.

Li X, Liu X, Xie J, Zhang Q, Yang Z, Schindlbacher A, Yang Y. 2021. Contribution of above ground litterfall and roots to the soil CO2 efflux of two sub-tropical Cunninghamia lanceolata and Castanopsis carlesii forests. Agricultural and Forest Meteorology 311:108671.

Litton CM, Raich JW, Ryan MG. 2007. Carbon allocation in forest ecosystems. Global Change Biology 13:2089–109.

Lorimer CG. 1980. Age Structure and Disturbance History of a Southern Appalachian Virgin Forest. Ecology 61:1169–84.

Maier CA, Albaugh TJ, Lee Allen H, Dougherty PM. 2004. Respiratory carbon use and carbon storage in mid-rotation loblolly pine (*Pinus taeda* L.) plantations: the effect of site resources on the stand carbon balance. Global Change Biology 10:1335–50.

Malhi Y, Baldocchi DD, Jarvis PG. 1999. The carbon balance of tropical, temperate and boreal forests. Plant Cell Environ 22:715–40.

Nave LE, Gough CM, Maurer KD, Bohrer G, Hardiman BS, Le Moine J, Munoz AB, Nadelhoffer KJ, Sparks JP, Strahm BD, Vogel CS, Curtis PS. 2011. Disturbance and the resilience of coupled carbon and nitrogen cycling in a north temperate forest. J Geophys Res 116:G04016.

Nave LE, Vance ED, Swanston CW, Curtis PS. 2010. Harvest impacts on soil carbon storage in temperate forests. Forest Ecology and Management 259:857–66.

Oishi AC, Miniat CF, Novick KA, Brantley ST, Vose JM, Walker JT. 2018. Warmer temperatures reduce net carbon uptake, but do not affect water use, in a mature southern Appalachian forest. Agricultural and Forest Meteorology 252:269–82.

Petrenko CL, Friedland AJ. 2015. Mineral soil carbon pool responses to forest clearing in Northeastern hardwood forests. GCB Bioenergy 7:1283–93.

Raich JW, Nadelhoffer KJ. 1989. Belowground Carbon Allocation in Forest Ecosystems: Global Trends. Ecology 70:1346–54.

Raich JW, Schlesinger WH. 1992. The global carbon dioxide flux in soil respiration and its relationship to vegetation and climate. Tellus B 44:81–99.

Ryan MG, Lavigne MB, Gower ST. 1997. Annual carbon cost of autotrophic respiration in boreal forest ecosystems in relation to species and climate. J Geophys Res 102:28871–83.

Savage JA, Clearwater MJ, Haines DF, Klein T, Mencuccini M, Sevanto S, Turgeon R, Zhang C. 2016. Allocation, stress tolerance and carbon transport in plants: how does phloem physiology affect plant ecology? Plant Cell & Environment 39:709–25.

Savage KE, Davidson EA, Abramoff RZ, Finzi AC, Giasson M-A. 2018. Partitioning soil respiration: quantifying the artifacts of the trenching method. Biogeochemistry 140:53–63.

Scharenbroch BC, Bockheim JG. 2008. Gaps and Soil C Dynamics in Old Growth Northern Hardwood–Hemlock Forests. Ecosystems 11:426–41.

Schroeer AE, Hendrick RL, Harrington TB. 1999. Root, ground cover, and litterfall dynamics within canopy gaps in a slash pine (*Pinus elliottii* Engelm.) dominated forest. Écoscience 6:548–55.

Subke J, Inglima I, Francesca Cotrufo M. 2006. Trends and methodological impacts in soil CO_2 efflux partitioning: A metaanalytical review. Global Change Biology 12:921–43.

Taskinen O, Ilvesniemi H, Kuuluvainen T, Leinonen K. Response of fine roots to an experimental gap in a boreal Picea abies forest.

Vargas R, Baldocchi DD, Bahn M, Hanson PJ, Hosman KP, Kulmala L, Pumpanen J, Yang B. 2011a. On the multi-temporal correlation between photosynthesis and soil CO_2 efflux: reconciling lags and observations. New Phytologist 191:1006–17.

Vargas R, Carbone MS, Reichstein M, Baldocchi DD. 2011b. Frontiers and challenges in soil respiration research: from measurements to model-data integration. Biogeochemistry 102:1–13.

Vose JM, Bolstad PV. 2007. Biotic and abiotic factors regulating forest floor CO2 flux across a range of forest age classes in the southern Appalachians. Pedobiologia 50:577–87.

Wilczynski CJ, Pickett STA. 1993. Fine root biomass within experimental canopy gaps: evidence for a below-ground gap. Journal of Vegetation Science 4:571–4.

Chapter 2: Canopy gap influence on partitioned components of soil respiration in a Southern Appalachian mixed-oak forest

Introduction

Forest ecosystems are vital global carbon (C) sinks which account for nearly half of stored terrestrial C and sequester approximately 30% of anthropogenic C emissions (Bonan 2008; Pan et al. 2011). The C balance of a forest system requires C uptake (sinks) to be greater than C release (sources) and is maintained by the rates of assimilation and disturbance (Lovett et al. 2006). Carbon assimilated by autotrophs is stored in plant biomass and soil until released as CO_2 from fire or metabolic waste, or by other disturbances leading to export (e.g. leaching, runoff, CH_4 efflux, biomass harvesting). Maintaining a thorough account of a forest's carbon budget, or the difference between the amount of C stored and the amount C released in a forest, is necessary for assessing how natural and anthropogenic disturbance influence a forest's C storage capacity (Houghton 2020; Fredlingstein et al. 2020).

Soil respiration (R_S) is the second largest C flux in terrestrial ecosystems and in some cases may even exceed net primary productivity (Raich & Schlesinger 1992; Baldocchi & Penuelas 2019). R_S is comprised of two primary components: heterotrophic respiration (R_H), from heterotrophic soil microbes, and autotrophic respiration (R_A), from roots and their associated mycorrhizal fungi (Kuzyakov 2006). Relative contributions of these two components can vary greatly by ecosystem and microclimate conditions (Raich & Tufekcioglu 2000; Hanson et al. 2000; Noormets et al. 2021), so distinguishing between these sources is necessary for an accurate accounting of the net C impact of R_S (Subke et al. 2006). A review of R_S partitioning in forest ecosystems by Hanson et al. (2000) found the heterotrophic component ranged seasonally from 5-100% of total respiration, with most studies reporting a 40-80% contribution to R_S. The

portion of R_S derived from R_A is heavily regulated by photosynthetic inputs (Hogberg et al. 2001) and may be susceptible to changes in aboveground gross primary productivity (Noormets et al. 2012).

Canopy gaps formed by downed or harvested trees play an important role in the ecological succession of forest communities and their function. The removal of overstory trees creates high-light conditions which promote understory growth among light-competitive species and increases soil temperature (T_S) and water availability (Denslow 1998; Royo & Carson 2006; Scharenbrock & Bockheim 2007; Muscolo et al. 2014). These increases are positively correlated with soil microbial activity, which regulates organic matter decomposition (Bunnell 1977) and nitrogen mineralization (Mladenoff 1987). The relationships between temperature and biochemical processes developed by van't Hoff (1896, 1898) and Arrhenius (1889) have since been extensively used to model R_S via T_S (Lloyd & Taylor 1994; Davidson et al. 2006; Savage et al. 2018).

The precise relationship between canopy gaps and R_S has been variable among previous studies; some studies have found canopy gaps to increase R_S compared to the surrounding unharvested forest (Scharenbrock & Bockheim 2008), some have found them to reduce R_S (Lewandowski et al. 2019), while others have reported no significant change in R_S between gaps and the surrounding forest (Stoffel et al. 2010). While R_S appears to be generally higher in the northern portions of gaps (Schatz et al. 2012), the apparent minimal response of R_S to canopy gaps may be indicative of the contributing components responding in ways that balance each other out.

The aim of this project was to identify changes to soil respiration and its heterotrophic and autotrophic components resulting from harvested canopy gaps. By implementing a forest-

edge-gap gradient in different size gaps, we hope to elucidate the influence canopy gaps have on belowground C dynamics. We hypothesized that R_S would be lowest at gap centers and increase continuously along the transect moving into the forest (Lewandowski et al. 2019; Schatz et al. 2012). The overstory vegetation at the gap edge provides a natural buffer between gap and intact forest, and roots from the living trees along the gap edge may provide R_A inputs further into the gap than the canopy extends. We expect to see a higher R_H in gaps than transition due to the favorable conditions for microbial activity and lower root productivity in the highly light-competitive environment (Denslow et al. 1998). We ask two main questions: 1) How does R_S and its components change over space due to gaps of different sizes; and 2) do component fluxes vary between gaps and reference conditions in a southern Appalachian mixed oak forest?

Methods

Site Description

This study took place at the Southern Appalachian Femelschlag Experiment (SAFE) located in the Pisgah National Forest, North Carolina (35°28'N, 82°40'W). For details regarding the study site and silvicultural manipulation, refer to Chapter 1. In June 2022, root exclusion collars (EC) were installed next to each PVC total soil CO_2 flux collar (non-exclusion collars, NEC) in six of the twelve treatment plots (see Chapter 1), including three including three small gaps (from 0.15 to 0.22 ha) and three large gaps (0.78 to 1.1 ha), and the three control plots. Treatment plots were selected for this study based on the logistical feasibility of installing root exclusion collars in rocky soils. Exclusion collars were constructed from carbonized steel tubes, 10 cm in diameter and 20 cm in length, with sharp, beveled bottom edges to sever roots. Variance in collar lengths due to beveling (19.3 to 20.4 cm) was accounted for in respiration calculations. Exclusion collars were installed as close to respiration collars as possible, and due

to the rocky nature the site the distance between EC and NEC collars ranged from 0.27 to 2.7 m (averaging 0.98 m).

R_S and R_H Measurements

Soil CO_2 flux was measured using a LI-COR LI-7810 infrared gas analyzer (LI-COR Biosciences, Lincoln, NE) with 8100-01S Smart Chamber for the total soil CO_2 flux treatments and a LI-COR LI-6800 infrared gas analyzer with 8100-102 10 cm survey chamber for the root exclusion treatments. Flux measurements were scaled to a common area to account for the size difference between chambers. Flux was measured simultaneously for total soil CO_2 flux and root exclusion treatments. CO_2 flux was measured for 90 s following a 10 s pre-purge to ensure equilibrium with ambient atmospheric CO_2. T_S and soil moisture were measured simultaneously with flux measurements. T_S was measured at 2.5 cm and 7 cm with paired soil thermometers. Soil moisture was measured at 6 cm depth using moisture meter (HH2 Moisture Meter, Delta-T Devices, Cambridge, UK) with soil moisture probe attachment (ML3 ThetaProbe Soil Moisture Sensor, Delta-T Devices, Cambridge, UK).

Soil CO_2 flux was measured eight times between June and December 2022: bi-weekly from June to August then monthly from September to December. All measurements were made between 8:00 am and 4:00 pm and no less than 24 hours after a significant rain event. Plot order was selected randomly each day, and measurements within each plot always started at collar 1 and moved in ascending order until each collar in the plot had been sampled.

Fine Root Biomass C

In Feb. 2023, root exclusion collars were removed from the ground with the internal soil kept intact and stored in plastic bags. All samples were returned to the laboratory and stored at 3°C until processed. To identify site-wide seasonal soil and root C and soil decay in exclusion

collars, soils were sifted through a 1 mm sieve and rocks and roots removed, washed, and roots sorted by size class (diameter <1 mm and >2 mm) and live verses dead based on texture and visual inspection (ArchMiller and Samuelson 2016). Roots and rocks were oven dried at 50°C for 72 hours before being weighed and roots ground for total C analysis.

Corrections to Measured Flux

The strong relationship between R_S and T_S has been well established in the literature (Lloyd & Taylor 1994; Savage et al. 2009). Per this relationship, the instantaneous temperature and log of the instantaneous flux measured at each sampling date was fitted to a linear model and the coefficients applied to Eq. 1:

$$R_t = e^{\alpha} e^{\beta T} \quad (1)$$

Where R_t (denoted R_s in total soil flux collars and R_e in exclusion collars) is the respiration ($\mu molCO_2 m^{-2} s^{-1}$), α is the intercept coefficient of the linear model, β is the slope coefficient of the linear model, and T is temperature (°C). The α and β coefficients are highly site-specific, so each individual collar was modeled independently. Modeled fits of individual collars ranged from $r^2 > 0.62$ to 0.99. T_S data from the iButtons was averaged by day, and daily average T_S for each collar was applied to Eq. 1 to get daily average CO_2 flux ($\mu molCO_2 m^{-2} d^{-1}$).

A concern often raised with the root exclusion collar method of partitioning R_S is the potential for water pooling within the root exclusion collars. In cases where soil moisture is significantly different within the collars than outside them, a water content correction can be applied to the CO_2 flux measured from the exclusion collars (Savage et al. 2009). At the end of the study, we took soil moisture measurements inside and directly outside each collar. Across all collars, the soil moisture differed by an average of 0.57±0.82%, and a linear regression between

the $\%H_2O$ inside and outside the collars gave an $r^2 > 0.62$. We therefore opted not to include a water content correction in our R_H calculations.

A major concern of using root exclusion collars to measure R_H is the superfluous CO_2 from the decay of recently severed roots (RSR). To account for this, the final root biomass from the exclusion collars was used to approximate starting root biomass and contribution of C from decomposition. The starting root biomass wasp calculated using Eq. 2 per Savage et al. (2018):

$$M_0 = \frac{M_1}{e^{-k(\frac{t}{365})}} \quad (2)$$

Where M_1 is the final root biomass (gC), M_0 is the starting root biomass (gC), k is the decay constant (d^{-1}), and t is time (d). A value of 0.26 was used for k based on a review of root decay constants in temperate hardwood forests published in the Fine Root Ecology Database (FRED 3.0; Iversen et al. 2021). M_0 was then used to determine the amount of C released as a result of root decomposition Eq. 3:

$$C_{loss} = (1 - a) * C * M_0(1 - e^{-kt}) \quad (3)$$

Where C_{loss} is the root C lost from decomposition (gC), a is the fraction of C incorporated into SOM (set at 0.22 by Jenkinson 1990), and C is the C concentration in roots. For each exclusion collar, the RSR-corrected R_H was calculated as Eq. 4:

$$R_h = R_e - C_{loss} \quad (4)$$

Autotrophic respiration was then calculated as the difference between total soil respiration and the heterotrophic partition Eq. 5:

$$R_a = R_s - R_h \quad (5)$$

Negative R_A Values

Since R_A was calculated as the difference between R_S and R_H, negative values can theoretically occur when CO_2 flux in the root exclusion collars is higher than in the total soil CO_2

flux collars. In our data set, 42.7% of daily R_A values were negative. The density of negative R_A values increased with decreasing seasonal T_S, but of our 38 collar pairs, 24 had at least one negative R_A measurement and 9 had exclusively negative R_A values throughout the study period. No consistency with gap size, plot, or collar location was found among these 20 pairs. Since negative R_A values have no biological relevance and are mathematical artifact, negative R_A values were replaced with zeroes for the purposes of data analysis.

Data Analysis

A full factorial mixed model analysis of variance with repeated measures was used to assess effects of collar location (n = 5), gap size (n = 2), time (d^{-1}; n = 165), and their interactions on daily average R_S, R_H, and R_A ($gCm^{-2}d^{-1}$). Within each gap size (small, large) the three nested treatment plots were treated as random effects and considered replicates. Using an AR(1) repeated structure, average respiration for each day included in the study (June 21 to December 2; n = 165) at each collar was included in the model. Due to the strong relationship between T_S and R_S, data were separated by season and summer days (June 21 to September 22, n = 94) were analyzed independent of fall days (September 23 to December 2, n = 71). To test for differences between treatment and control plots, collars in each treatment plot were grouped by gap (collars 4 and 5) and transition zone (collars 1, 2, and 3), and the three collars in each control plot grouped as controls. Daily average R_S, R_H, R_A and T_S (separated by season) for each collar was averaged by zone, giving a gap average and transition zone average for each treatment plot and a control average for each control plot. Due to the lack of independence between gap and transition zones, T-tests were performed to find differences between controls and gaps, controls and transition zones, and gaps and transition zones. All statistical analyses were performed in R (4.3.1) and JMP Version 16 (SAS Institute Inc., Cary, NC).

Results

Soil Respiration and Microclimate

Daily average R_S ranged from 15.764 $gCm^{-2}d^{-1}$ in summer to 0.298 $gCm^{-2}d^{-1}$ in fall and varied significantly by season (Figure 2.1; $P < 0.0001$). R_S did not differ significantly by gap size or collar location in either summer or fall (Figure 2.2, Figure 2.3), but a gap size by location interaction was significant in both seasons (Table 2.1). A pairwise comparison of these interaction effects revealed no significant interactions between any individual collars or gap sizes. No significant difference was observed between R_S in control plots and gaps or transition zones (Figure 2.3).

Daily average T_S near the collars ranged from 0.13°C in fall to 27.5°C in summer, averaging 16.6°C across the duration of the study (Figure 2.4). Large gaps averaged 0.52°C warmer than small gaps, with that difference being more pronounced during warmer months. Average T_S increased linearly from collar 1 to 4, with collar 5 closely mirroring collar 3 (Table 2.2). T_S in the gaps was significantly greater than in the controls, averaging 20.9°C and 19.5°C respectively in the summer months ($P = 0.0172$) and 12.5°C and 10.9°C respectively in the fall months ($P = 0.0112$). T_S did not differ significantly between transition zones and controls in either season ($P = 0.1115$ in summer; $P = 0.1081$ in fall) but was higher in gaps than in transition zones for both summer ($P = 0.0311$) and fall ($P = 0.0402$). No significant difference in T_S was observed between exclusion and total soil flux collars ($r^2 > 0.88$; $P < 0.0001$;).

Soil moisture near the collars ranged from 3% to 45%, averaging 18.0% across all sampling dates. Small gaps had significantly higher soil moisture than large gaps ($P < 0.0001$; Figure 2.5). Soil moisture was generally higher in the summer months, peaking in late-July. The highest recorded soil moisture measurements occurred in November/December, possibly due to

the influence of seasonal snowfall. Average soil moisture was slightly higher in gaps (20.9%) than in transition zones (17.1%; P = 0.3079) or controls (18.0%; P = 0.2645), but these differences were not significant. No trend in soil moisture was observed along the gap gradients in small (P = 0.3179) or large (P = 0.1939) gaps (Figure 2.6).

Partitioned Soil Respiration

The contribution of R_H to R_S ranged from 46.4% to 100% in summer and 8.6% to 100% in fall, averaging 86.1% and 87.7%, respectively. The contribution of R_A to R_S ranged from 0% to 53.6% in summer and 0% to 91.4% in fall, averaging 13.9% and 12.3% respectively (Figure 2.1).

No consistent gap-induced effect was found for R_H or R_A. Time (d^{-1}) was significant for R_H in both summer ($P < 0.001$) and fall ($P < 0.0001$) and for R_A in fall ($P < 0.05$) but not summer ($P = 0.77$; Table 2.1). Gaps were not found to be significantly different from control plots or transition zones (Figure 2.3) for either R_H or R_A.

Root biomass within individual exclusion collars ranged from 0.958g to 30.940g but did not follow any consistent spatial trends by collar location ($P > 0.63$), zone ($P > 0.16$), or gap size ($P > 0.27$). A linear regression revealed no significant correlation between root biomass within the exclusion collars and raw CO_2 flux ($r^2 = 0.01$, $P > 0.5$). Among all collars, 31.8% of roots were <2 mm and 68.2% were >2 mm in diameter and 59.1% of roots were classified as "live" and 40.9% as "dead".

Discussion

Seasonal Patterns

Strong seasonal differences resulting from the close relationship between R_S and T_S were seen in R_S, R_H, and R_A. Across all locations and gap sizes, R_S and R_H decreased considerably

during the last week of September correlating with an equivalent decrease in T_S. While our study did not include the entire growing season, our data captures 94 summer days and 71 fall days. Despite seasonal differences in respiration across all partitions, the relative contribution of each individual location remained consistent through the measurement period; that is, we saw high inter-collar variability but low intra-collar variability.

How Do R_S and R_H Differ Across Gap Transects?

Across our 165-day measurement period, we saw no evidence of a gap-based influence on R_S or R_H. Patterns in R_S and R_H flux across the gap gradient varied between replicate plots due to the heterogeneous nature of our field site, but overall trends revealed no consistent difference between respiration collars along the gap-forest transect or between gaps and the undisturbed control plots. These findings are consistent with studies comparing R_S between harvested canopy gaps and unharvested controls in the Flambeau River State Forest, a mature northern hardwood forest (Stoffel et al. 2010; Forrester et al. 2013; Perreault et al. 2021). However, a number of studies have observed reduced R_S in response to canopy disturbance across a wide range of biomes and treatment conditions (Edwards and Ross-Todd 1983; Mattson and Swank 1989; Strigl and Wickland 1998; Li et al. 2012; Moore et al. 2013; Kurth et al. 2014).

The variety of sources contributing to R_H make it difficult to measure and cause estimates to have high uncertainty. The manner in which R_H responds following a disturbance depends on the disturbance agent, severity, and extent of legacy C removed by the event (Harmon et al. 2011). Microbial-sourced R_H tends to increase exponentially with soil temperature across its range but exhibits a more complex relationship with soil moisture. We expected the higher soil temperatures to enhance R_H in the gaps but saw no change relative to the unharvested locations. The elevated temperatures may have been offset by reduced overstory litterfall in the gaps; a

reduction of available labile C inputs would limit microbial respiration and potentially cause lower R_H than would be expected from the temperature relationship alone (Davidson et al. 2012)

The autotrophic component of R_S is mediated by the allocation of gross primary product (i.e. photosynthate) to roots and mycorrhizae (Ryan et al. 1997; Harmon et al. 2004; Litton et al. 2007), so the disruption of C assimilation (Baldocchi 2008) or phloem transport (Savage et al. 2016) should lead to a reduction in R_A within individual trees. In the growing season following a stem-girdling treatment of early successional species in a temperate secondary forest, R_S declined by up to 39% compared to an undisturbed control plot (Nave et al. 2011), and in the first three years following an outbreak of mountain pine beetles (*Dendroctonus ponderosae*) in a lodgepole pine (*Pinus ponderosa*) dominated subalpine forest, Moore et al. (2013) observed a ~40% decline in R_S compared to an unaffected control plot.

We speculate that a contributing factor to our observed lack in differentiation between disturbed and undisturbed R_S may be the growth of understory vegetation growing in our harvested plots. The current study took place three years post-harvest, and with no management of understory growth in the gaps since harvest, the herbaceous vegetation was dense enough to frequently inhibit traversal through the plots. This dense understory vegetation may have contributed to R_S in three ways: 1) the allocation of carbon belowground to increase R_A (Ryan et al. 1997), 2) a perennial input of fresh litter to fuel soil heterotrophs (Malhi et al. 1999), and/or 3) provide shade to the soil surface, thereby lowering T_S and associated respiratory activity (Lloyd and Taylor 1994). While we cannot verify these explanation within the confines of the current study, this does present an opportunity for future studies to thoroughly explore the ecological mechanisms regulating soil respiration in mature temperate forests.

Negative R_A Values

Negative R_A values are a common byproduct of using root exclusion collars to partition R_S (Savage et al. 2018; Brown and Markewitz 2018). In a partitioning study across six Southeast US pine plantations using root exclusion collars, 51 of 161 partitioned measurements had negative R_A values (Brown and Markewitz 2018). The theoretical basis of the method assumes the exclusion and total soil flux collars will be measured under identical conditions, such that the input of root respiration is the only difference between them. Savage et al. (2018) notes that the reduction of C allocated to roots in the fall and subsequent reduction in R_A can lead to seasonal trends of R_S fluxes dropping below their paired R_H fluxes. Comparatively, 63.2% of our collar pairs had at least one negative R_A estimation, and 23.7% had negative R_A estimations for the entire duration of our study. The large difference in respiration between closely paired collars indicates a high degree of spatial variability at our study site. In comparing trends between R_S and litterfall among a range of forest types, Davidson et al. (2002) noted that mature hardwood forests were the only forest type to not have a significant linear trend between R_S and litterfall. While the precise cause of this phenomenon is still unclear, our results point to environmental heterogeneity as a potential contributing factor.

Conclusion

In this study, we attempted to elucidate the effect of harvested canopy gaps on soil respiration (R_S) and its heterotrophic (R_H) and autotrophic (R_A) components by measuring respiration along a gap-forest transect in replicated harvested plots. Seasonal trends in R_S, R_H, and R_A largely followed T_S. We observed no consistent difference in R_S or either partition along the gap gradient or between harvested and control plots despite seeing a significant trend of increasing T_S from the intact forest into the gaps. While the influence of canopy gaps on R_S is

inconsistent and varies widely by study site, we point to the three years of understory growth within the gaps as a potential contributing factor to the similar levels of respiration between harvested and unharvested locations. Mature temperate hardwood forests are noted for not following the trends in C dynamics typically seen in other forest types (Davidson et al. 2002), so understanding how canopy disturbance influences soil respiration in Southern Appalachian mixed-oak forests will help in evaluating the C budget trade-offs of harvesting regimes.

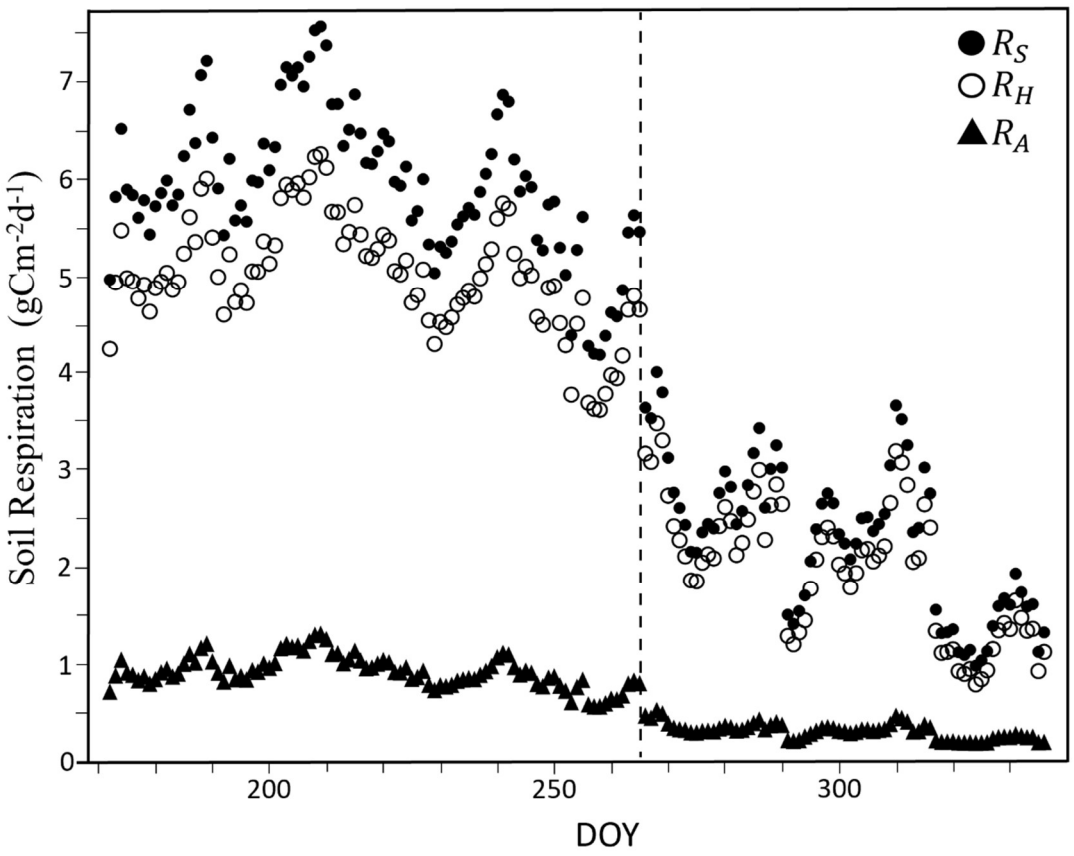

Figure 2.1 Daily average soil respiration ($gCm^{-2}d^{-1}$) from June 21 to December 2, 2022, for total soil respiration (R_S), heterotrophic respiration (R_H), and autotrophic respiration (R_A). Each point represents the site-wide average for a given day. Dashed line represents the delineation between summer to fall.

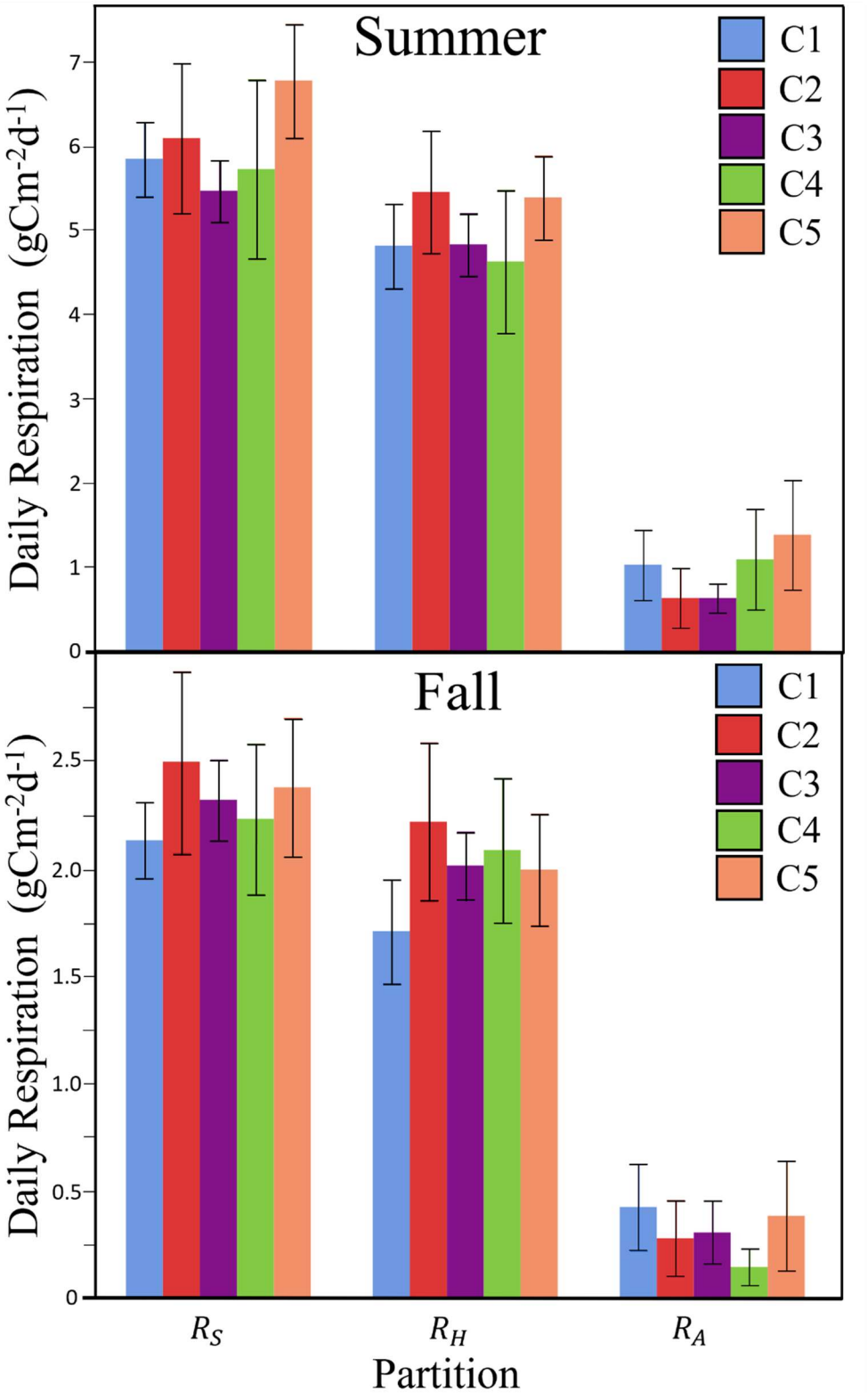

Figure 2.2 Average R_S, R_H, and R_A ($gCm^{-2}d^{-1}$) for each collar location (Collar 1 – Collar 5; C1 – C5) in summer (June 21 to September 22) and fall (September 23 to December 2), 2022. Error bars indicate one standard error from the mean.

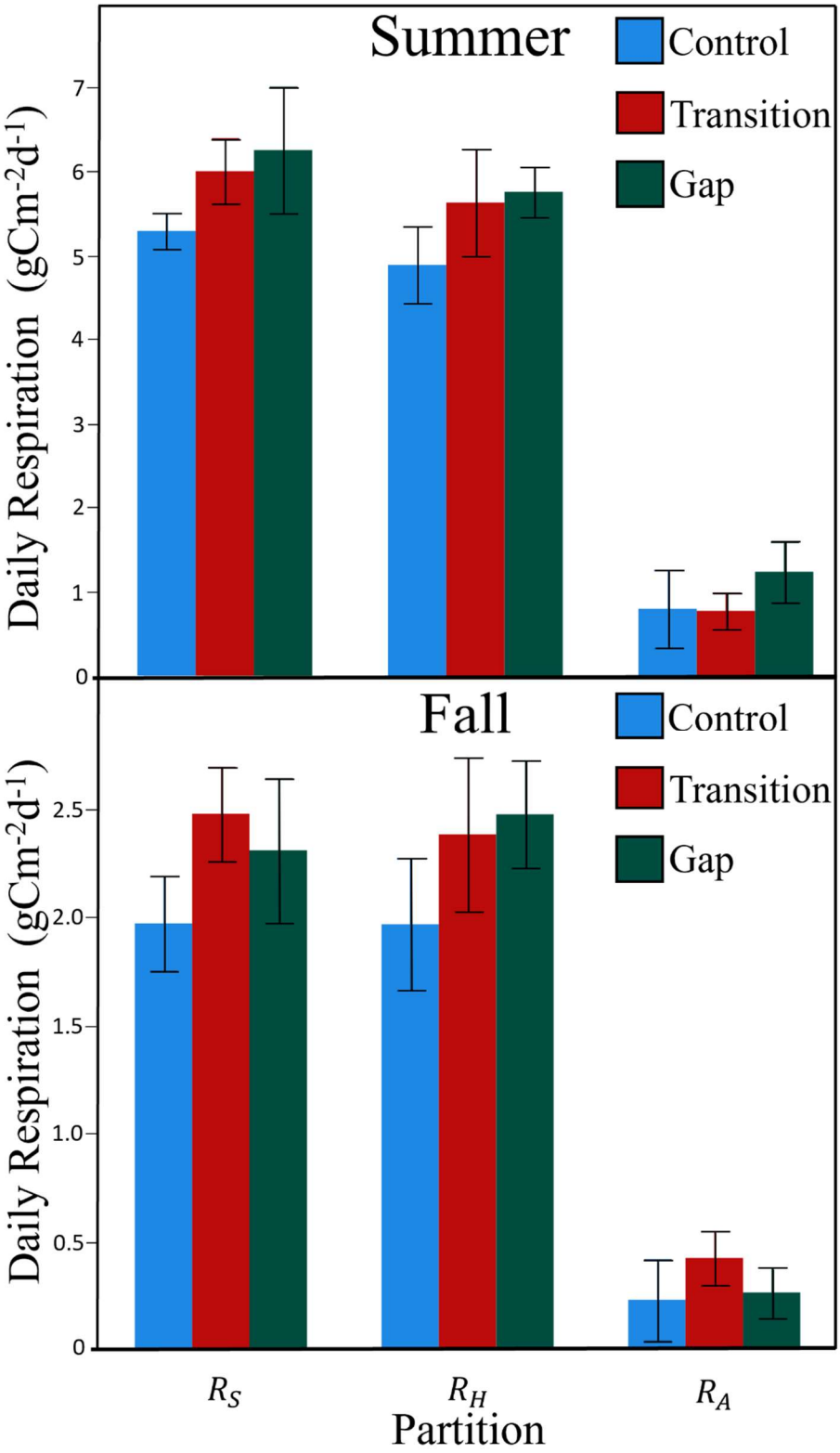

Figure 2.3 Average R_S, R_H, and R_A ($gCm^{-2}d^{-1}$) for the controls, transition zones, and gaps in summer (June 21 to September 22) and fall (September 23 to December 2), 2022. Error bars indicate one standard error from the mean.

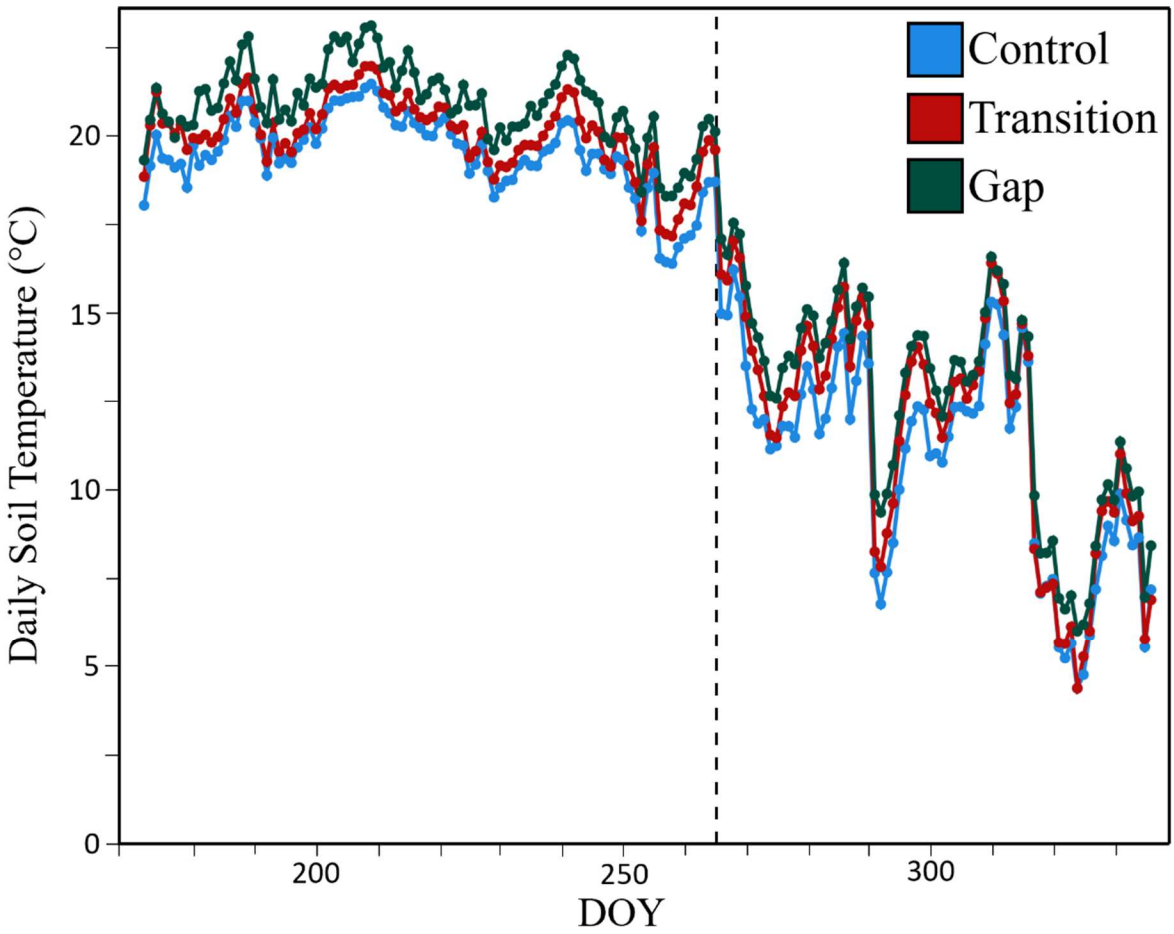

Figure 2.4 Daily average T_S (°C) in the controls, transition zones, and gaps. Dashed line represents the delineation between summer and fall.

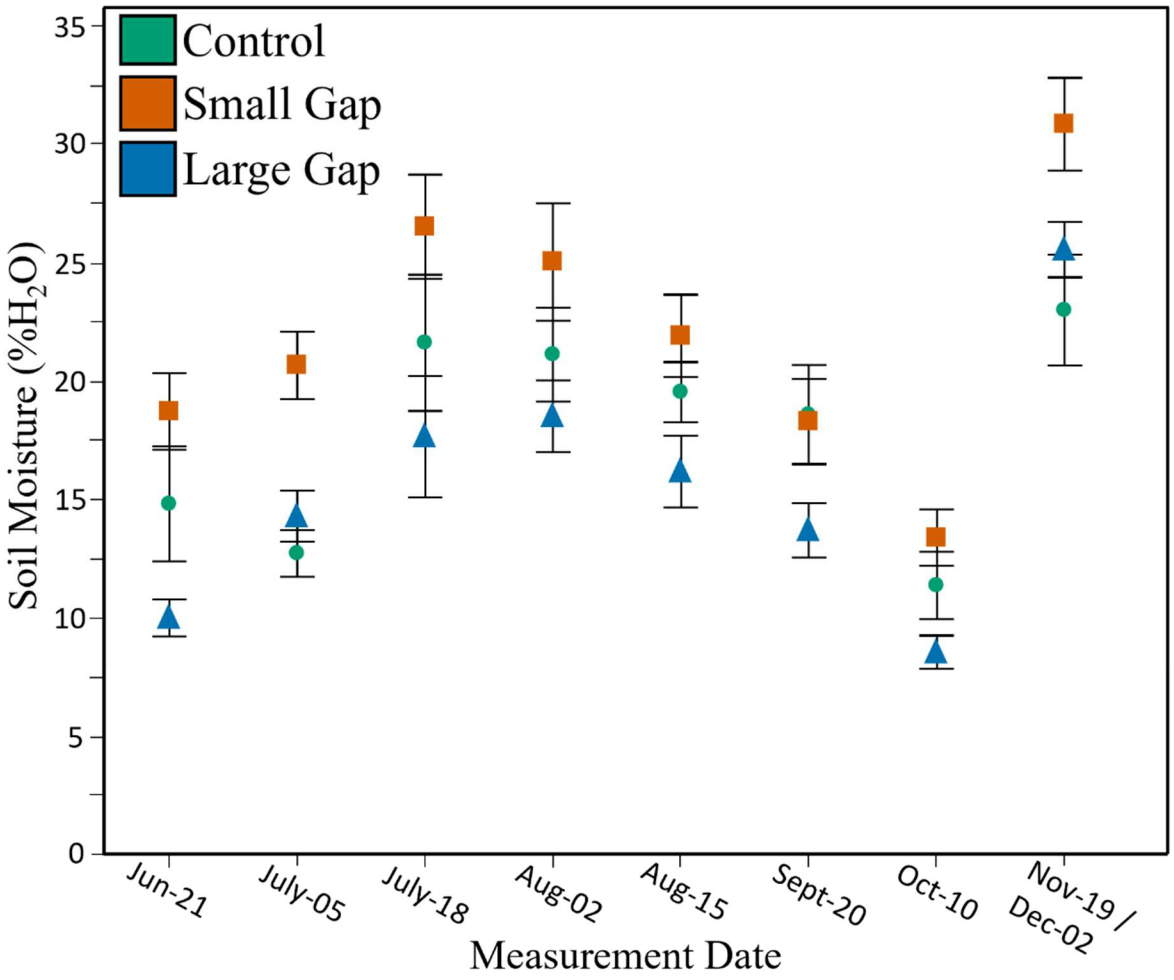

Figure 2.5 Average discrete soil moisture (% H_2O) for control plots, small gaps, and large gaps at each sampling date. Error bars represent one standard error from the mean.

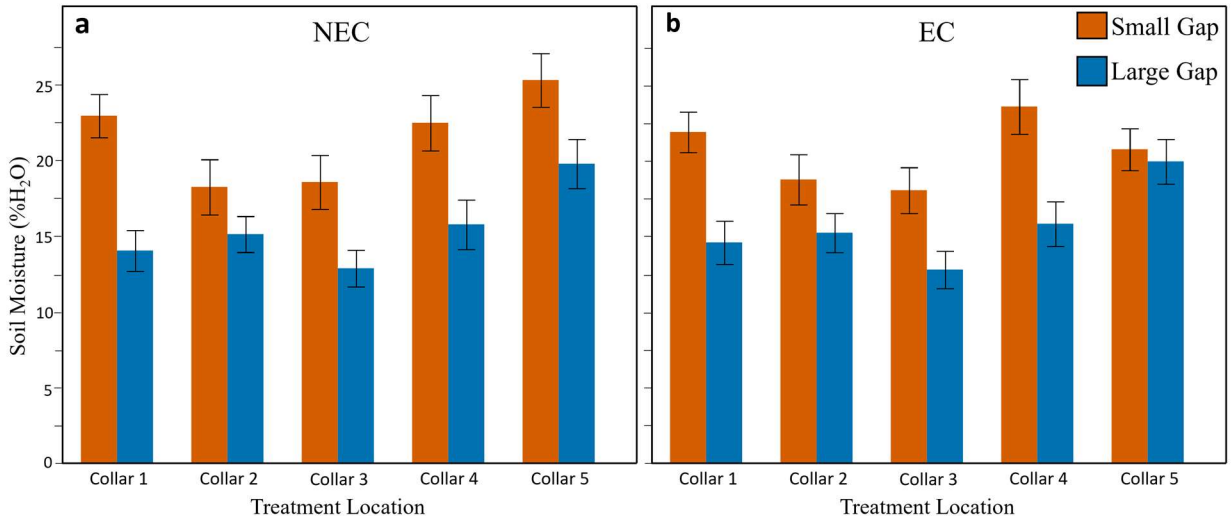

Figure 2.6 Average discrete soil moisture (% H_2O) across all sampling dates for each total soil CO_2 flux (**a**; non-exclusion collars, NEC) and root exclusion (**b**; exclusion collar, EC) collar location in small gaps and large gaps.

Table 2.1 Significant differences between treatment plot collar locations (n = 5), gap size (large, small), time (represented as differences in daily average respiration between days within each season, n = 94 and n = 71 for summer and fall, respectively), and interactions between those factors for R_S, R_H, and R_A in summer and fall. *P* values obtained from a mixed model ANOVA with repeated measures to assess the effects of treatment factors and their interactions on R_S, R_H, and R_A. Tests were conducted separately for summer and fall.

Treatment factor	Summer			Fall		
	R_S	R_H	R_A	R_S	R_H	R_A
Collar location	0.8310	0.8136	0.7725	0.6869	0.8952	0.5690
Gap size	0.7346	0.2293	0.2516	0.9530	0.4616	0.3318
Time	**0.0053**	**0.0002**	0.7749	**<0.0001**	**<0.0001**	**0.0035**
Location * gap size	**0.0426**	0.1979	0.6802	**0.0157**	0.5875	0.2164
Location * time	0.5627	0.3028	0.3822	0.8618	0.8025	0.3721
Gap size * time	0.7792	0.2683	0.9173	0.7097	0.3511	**0.0130**
Location * gap size * time	0.6472	0.3371	0.9454	0.0630	0.1877	0.2133

Bold indicates a significant difference at $\alpha < 0.05$

Table 2.2 Pairwise comparisons of mean soil temperature (T_S), total soil respiration (R_S), heterotrophic respiration (R_H), and autotrophic respiration (R_A) at each collar location by gap size and season. T_S values (SE) in °C. Respiration values (SE) in $gCm^{-2}d^{-1}$.

Season	Treatment		Collar 1	Collar 2	Collar 3	Collar 4	Collar 5
			15 m in forest	7.5 m in forest	Gap edge	7.5 m in gap	15 m in gap
Summer	Control	T_S	19.4 (0.07)	19.5 (0.07)	19.6 (0.07)	–	–
		R_S	5.09 (0.06)	6.02 (0.13)	4.74 (0.05)	–	–
		R_H	4.16 (0.06)	5.23 (0.05)	5.25 (0.10)	–	–
		R_A	0.93 (0.02)	1.16 (0.08)	0.31 (0.36)	–	–
	Small Gap	T_S	19.6 (0.07)	20.1 (0.11)	20.2 (0.06)	20.6 (0.08)	20.4 (0.06)
		R_S	5.98 (0.06)	8.54 (0.20)	5.14 (0.04)	4.12 (0.08)	6.55 (0.09)
		R_H	6.97 (0.16)	7.86 (0.19)	4.20 (0.03)	4.81 (0.05)	6.93 (0.09)
		R_A	0.46 (0.04)	0.67 (0.01)	0.94 (0.02)	0.57 (0.05)	0.95 (0.04)
	Large Gap	T_S *	19.6 (0.07)^{A}	20.1 (0.07)^{A}	20.9 (0.07)^{AB}	22.0 (0.11)^{B}	20.7 (0.07)^{AB}
		R_S	6.46 (0.11)	4.52 (0.04)	6.51 (0.08)	7.32 (0.16)	6.99 (0.12)
		R_H	4.99 (0.11)	4.97 (0.06)	6.06 (0.07)	6.04 (0.13)	5.23 (0.10)
		R_A	1.70 (0.10)	0.09 (0.01)	0.66 (0.03)	1.62 (0.10)	1.82 (0.11)
Fall	Control	T_S	10.9 (0.22)	10.7 (0.22)	11.1 (0.21)	–	–
		R_S	1.69 (0.05)	2.37 (0.09)	1.85 (0.05)	–	–
		R_H	1.72 (0.05)	2.09 (0.05)	2.09 (0.08)	–	–
		R_A	0.07 (0.01)	0.49 (0.04)	0.13 (0.01)	–	–
	Small Gap	T_S	10.5 (0.23)	11.6 (0.29)	12.2 (0.21)	12.2 (0.22)	12.2 (0.20)
		R_S	2.37 (0.06)	3.92 (0.12)	2.56 (0.06)	1.93 (0.05)	1.99 (0.06)
		R_H	2.59 (0.12)	3.55 (0.14)	2.03 (0.04)	2.34 (0.05)	2.88 (0.10)
		R_A	0.35 (0.04)	0.38 (0.03)	0.66 (0.04)	0.10 (0.01)	0.01 (0.004)
	Large Gap	T_S *	11.1 (0.23)^{A}	11.8 (0.25)^{AB}	13.1 (0.23)^{B}	12.9 (0.25)^{B}	12.6 (0.21)^{AB}
		R_S	2.34 (0.07)	1.68 (0.05)	2.57 (0.07)	2.54 (0.10)	2.78 (0.08)
		R_H	1.92 (0.09)	2.25 (0.06)	2.70 (0.08)	2.53 (0.09)	2.16 (0.08)
		R_A	0.81 (0.05)	0.00 (0.00)	0.13 (0.01)	0.19 (0.02)	0.75 (0.05)

* Indicates the presence of significant differences between collar locations
Upper case letters indicate individual collar differences at $\alpha = 0.05$

REFERENCES

ArchMiller A, Samuelson L. 2016. Partitioning Longleaf Pine Soil Respiration into Its Heterotrophic and Autotrophic Components through Root Exclusion. Forests 7:39.

Arrhenius S. Über die Dissociationswärme und den Einfluss der Temperatur auf den Dissociationsgrad der Elektrolyte.

Baldocchi D. 2008. 'Breathing' of the terrestrial biosphere: lessons learned from a global network of carbon dioxide flux measurement systems. Aust J Bot 56:1.

Baldocchi D, Penuelas J. 2019. The physics and ecology of mining carbon dioxide from the atmosphere by ecosystems. Global Change Biology 25:1191–7.

Bonan GB. 2008. Forests and Climate Change: Forcings, Feedbacks, and the Climate Benefits of Forests. Science 320:1444–9.

Brown R, Markewitz D. 2018. Soil heterotrophic respiration: Measuring and modeling seasonal variation and silvicultural impacts. Forest Ecology and Management 430:594–608.

Bunnell FL, Tait DEN, Flanagan PW, Van Clever K. 1977. Microbial respiration and substrate weight loss—I. Soil Biology and Biochemistry 9:33–40.

Davidson EA, Janssens IA, Luo Y. 2006. On the variability of respiration in terrestrial ecosystems: moving beyond Q_{10}. Global Change Biology 12:154–64.

Davidson EA, Samanta S, Caramori SS, Savage K. 2012. The Dual Arrhenius and Michaelis–Menten kinetics model for decomposition of soil organic matter at hourly to seasonal time scales. Global Change Biology 18:371–84.

Davidson EA, Savage K, Bolstad P, Clark DA, Curtis PS, Ellsworth DS, Hanson PJ, Law BE, Luo Y, Pregitzer KS, Randolph JC, Zak D. 2002. Belowground carbon allocation in forests estimated from litterfall and IRGA-based soil respiration measurements. Agricultural and Forest Meteorology 113:39–51.

Denslow JS, Ellison AM, Sanford RE. 1998. Treefall gap size effects on above- and below-ground processes in a tropical wet forest. Journal of Ecology 86:597–609.

Edwards NT, Ross-Todd BM. 1983. Soil Carbon Dynamics in a Mixed Deciduous Forest Following Clear-Cutting with and without Residue Removal. Soil Science Soc of Amer J 47:1014–21.

Forrester JA, Mladenoff DJ, Gower ST. 2013. Experimental Manipulation of Forest Structure: Near-Term Effects on Gap and Stand Scale C Dynamics. Ecosystems 16:1455–72.

Friedlingstein P, O'Sullivan M, Jones MW, Andrew RM, Hauck J, Olsen A, Peters GP, Peters W, Pongratz J, Sitch S, Le Quéré C, Canadell JG, Ciais P, Jackson RB, Alin S, Aragão LEOC, Arneth A, Arora V, Bates NR, Becker M, Benoit-Cattin A, Bittig HC, Bopp L,

Bultan S, Chandra N, Chevallier F, Chini LP, Evans W, Florentie L, Forster PM, Gasser T, Gehlen M, Gilfillan D, Gkritzalis T, Gregor L, Gruber N, Harris I, Hartung K, Haverd V, Houghton RA, Ilyina T, Jain AK, Joetzjer E, Kadono K, Kato E, Kitidis V, Korsbakken JI, Landschützer P, Lefèvre N, Lenton A, Lienert S, Liu Z, Lombardozzi D, Marland G, Metzl N, Munro DR, Nabel JEMS, Nakaoka S-I, Niwa Y, O'Brien K, Ono T, Palmer PI, Pierrot D, Poulter B, Resplandy L, Robertson E, Rödenbeck C, Schwinger J, Séférian R, Skjelvan I, Smith AJP, Sutton AJ, Tanhua T, Tans PP, Tian H, Tilbrook B, van der Werf G, Vuichard N, Walker AP, Wanninkhof R, Watson AJ, Willis D, Wiltshire AJ, Yuan W, Yue X, Zaehle S. 2020. Global Carbon Budget 2020. Earth Syst Sci Data 12:3269–340.

Grover ZS, Forrester JA, Keyser TL, King JS, Altman J. 2023. Growth response, climate sensitivity and carbon storage vary with wood porosity in a southern Appalachian mixed hardwood forest. Agricultural and Forest Meteorology 332:109358.

Hanson PJ, Edwards NT, Garten CT, Andrews JA. Separating root and soil microbial contributions to soil respiration: A review of methods and observations.

Harmon ME, Bible K, Ryan MichaelG, Shaw DavidC, Chen H, Klopatek J, Li X. 2004. Production, Respiration, and Overall Carbon Balance in an Old-growth Pseudotsuga-Tsuga Forest Ecosystem. Ecosystems. http://link.springer.com/10.1007/s10021-004-0140-9.

Harmon ME, Bond-Lamberty B, Tang J, Vargas R. 2011. Heterotrophic respiration in disturbed forests: A review with examples from North America. J Geophys Res 116:G00K04.

Hoff JH van't, Cohen E, Ewan T. 1896. Studies in Chemical Dynamics. F. Muller

Hoff JH van't, Lehfeldt RA. 1899. Lectures on theoretical and physical chemistry, by Dr. J. H. van't Hoff, tr. by Dr. R. A. Lehfeldt. London,: E. Arnold http://www.biodiversitylibrary.org/bibliography/17742.

Högberg P, Nordgren A, Buchmann N, Taylor AFS, Ekblad A, Högberg MN, Nyberg G, Ottosson-Löfvenius M, Read DJ. 2001. Large-scale forest girdling shows that current photosynthesis drives soil respiration. Nature 411:789–92.

Houghton RA. 2020. Terrestrial fluxes of carbon in GCP carbon budgets. Global Change Biology 26:3006–14.

Jenkinson DS, Andrew SPS, Lynch JM, Goss MJ, Tinker PB, Greenwood DJ, Nye PH, Walker A. 1997. The turnover of organic carbon and nitrogen in soil. Philosophical Transactions of the Royal Society of London Series B: Biological Sciences 329:361–8.

Kurth VJ, Bradford JB, Slesak RA, D'Amato AW. 2014. Initial soil respiration response to biomass harvesting and green-tree retention in aspen-dominated forests of the Great Lakes region. Forest Ecology and Management 328:342–52.

Kuzyakov Y. 2006. Sources of CO2 efflux from soil and review of partitioning methods. Soil

Biology and Biochemistry 38:425–48.

Lewandowski TE, Forrester JA, Mladenoff DJ, D'Amato AW, Fassnacht DSA, Padley E, Martin KJ. 2019. Do biological legacies moderate the effects of forest harvesting on soil microbial community composition and soil respiration. Forest Ecology and Management 432:298–308.

Li Q, Chen J, Moorhead DL. 2012. Respiratory carbon losses in a managed oak forest ecosystem. Forest Ecology and Management 279:1–10.

Litton CM, Raich JW, Ryan MG. 2007. Carbon allocation in forest ecosystems. Global Change Biology 13:2089–109.

Lloyd J, Taylor JA. 1994. On the Temperature Dependence of Soil Respiration. Functional Ecology 8:315.

Lovett GM, Cole JJ, Pace ML. 2006. Is Net Ecosystem Production Equal to Ecosystem Carbon Accumulation? Ecosystems 9:152–5.

Malhi Y, Baldocchi DD, Jarvis PG. 1999. The carbon balance of tropical, temperate and boreal forests. Plant Cell Environ 22:715–40.

Mattson KG, Swank WT. 1989. Soil and detrital carbon dynamics following forest cutting in the Southern Appalachians. Biol Fert Soils 7:247–53.

Mladenoff DJ. 1987. Dynamics of Nitrogen Mineralization and Nitrification in Hemlock and Hardwood Treefall Gaps. Ecology 68:1171–80.

Moore DJP, Trahan NA, Wilkes P, Quaife T, Stephens BB, Elder K, Desai AR, Negron J, Monson RK. 2013. Persistent reduced ecosystem respiration after insect disturbance in high elevation forests. Penuelas J, editor. Ecol Lett 16:731–7.

Muscolo A, Bagnato S, Sidari M, Mercurio R. 2014. A review of the roles of forest canopy gaps. Journal of Forestry Research 25:725–36.

Nave LE, Gough CM, Maurer KD, Bohrer G, Hardiman BS, Le Moine J, Munoz AB, Nadelhoffer KJ, Sparks JP, Strahm BD, Vogel CS, Curtis PS. 2011. Disturbance and the resilience of coupled carbon and nitrogen cycling in a north temperate forest. J Geophys Res 116:G04016.

Noormets A, Bracho R, Ward E, Seiler J, Strahm B, Lin W, McElligott K, Domec J, Gonzalez-Benecke C, Jokela EJ, Markewitz D, Meek C, Miao G, McNulty SG, King JS, Samuelson L, Sun G, Teskey R, Vogel J, Will R, Yang J, Martin TA. 2021. Heterotrophic Respiration and the Divergence of Productivity and Carbon Sequestration. Geophysical Research Letters 48:e2020GL092366.

Noormets A, McNulty SG, Domec J, Gavazzi M, Sun G, King JS. 2012. The role of harvest residue in rotation cycle carbon balance in loblolly pine plantations. Respiration

partitioning approach. Global Change Biology 18:3186–201.

Pan Y, Birdsey RA, Fang J, Houghton R, Kauppi PE, Kurz WA, Phillips OL, Shvidenko A, Lewis SL, Canadell JG, Ciais P, Jackson RB, Pacala SW, McGuire AD, Piao S, Rautiainen A, Sitch S, Hayes D. 2011. A Large and Persistent Carbon Sink in the World's Forests. Science 333:988–93.

Perreault L, Forrester JA, Mladenoff DJ, Gower ST. 2021. Linking deadwood and soil GHG fluxes in a second growth north temperate deciduous forest (Upper Midwest USA). Biogeochemistry 156:177–94.

Raich JW, Schlesinger WH. 1992. The global carbon dioxide flux in soil respiration and its relationship to vegetation and climate. Tellus B 44:81–99.

Raich JW, Tufekciogul A. 2000. Vegetation and soil respiration: Correlations and controls. Biogeochemistry 48:71–90.

Royo AA, Carson WP. 2006. On the formation of dense understory layers in forests worldwide: consequences and implications for forest dynamics, biodiversity, and succession. Can J For Res 36:1345–62.

Ryan MG, Lavigne MB, Gower ST. 1997. Annual carbon cost of autotrophic respiration in boreal forest ecosystems in relation to species and climate. J Geophys Res 102:28871–83.

Savage JA, Clearwater MJ, Haines DF, Klein T, Mencuccini M, Sevanto S, Turgeon R, Zhang C. 2016. Allocation, stress tolerance and carbon transport in plants: how does phloem physiology affect plant ecology? Plant Cell & Environment 39:709–25.

Savage K, Davidson EA, Richardson AD, Hollinger DY. 2009. Three scales of temporal resolution from automated soil respiration measurements. Agricultural and Forest Meteorology 149:2012–21.

Savage KE, Davidson EA, Abramoff RZ, Finzi AC, Giasson M-A. 2018. Partitioning soil respiration: quantifying the artifacts of the trenching method. Biogeochemistry 140:53–63.

Scharenbroch BC, Bockheim JG. 2007. Impacts of forest gaps on soil properties and processes in old growth northern hardwood-hemlock forests. Plant Soil 294:219–33.

Scharenbroch BC, Bockheim JG. 2008. Gaps and Soil C Dynamics in Old Growth Northern Hardwood–Hemlock Forests. Ecosystems 11:426–41.

Schatz JD, Forrester JA, Mladenoff DJ. 2012. Spatial Patterns of Soil Surface C Flux in Experimental Canopy Gaps. Ecosystems 15:616–23.

Stoffel JL, Gower ST, Forrester JA, Mladenoff DJ. 2010. Effects of winter selective tree harvest on soil microclimate and surface CO2 flux of a northern hardwood forest. Forest Ecology and Management 259:257–65.

Striegl RG, Wickland KP. 1998. Effects of a clear-cut harvest on soil respiration in a jack pine – lichen woodland. 28.

Subke J, Inglima I, Francesca Cotrufo M. 2006. Trends and methodological impacts in soil CO_2 efflux partitioning: A metaanalytical review. Global Change Biology 12:921–43.

APPENDICES

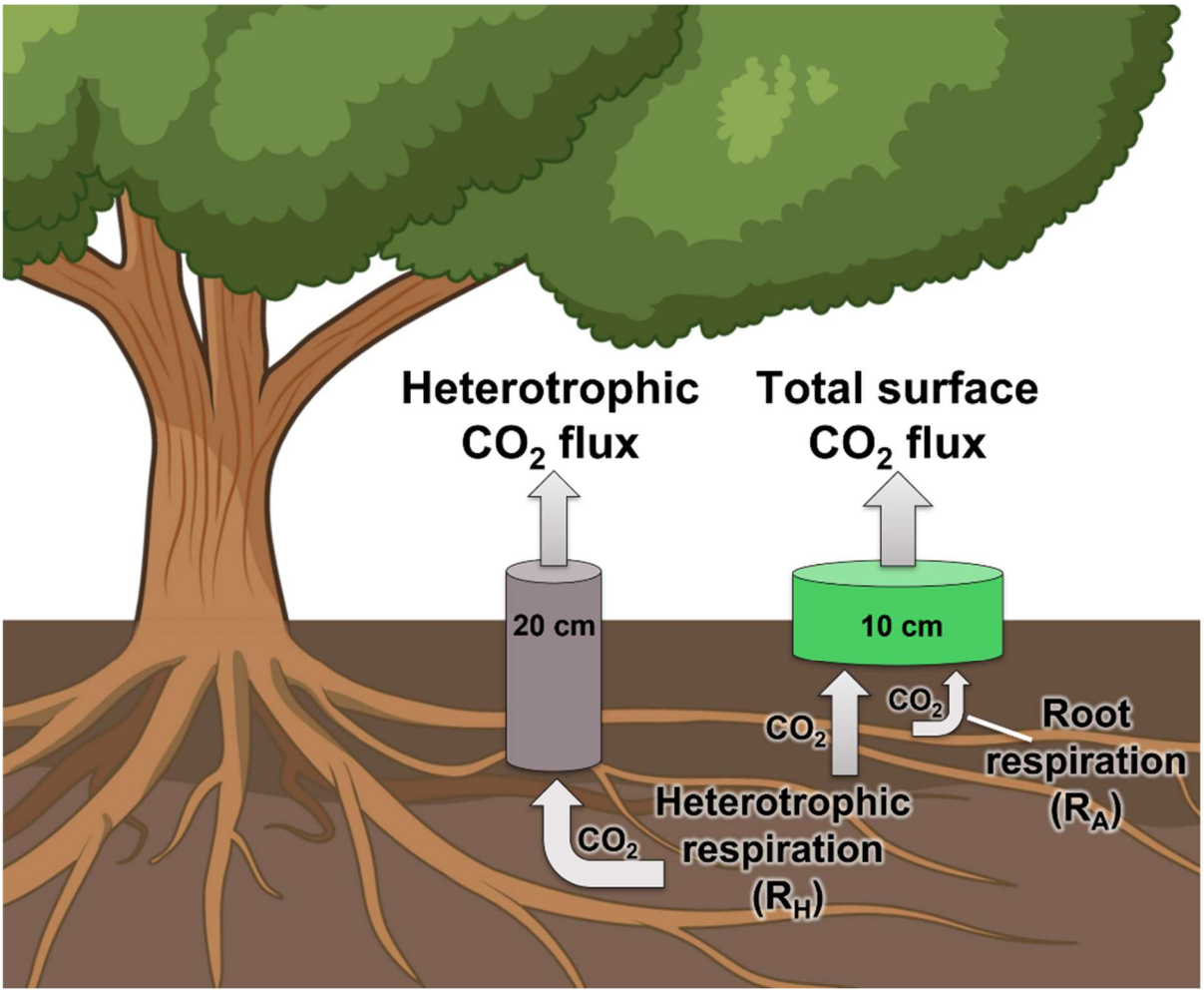

Figure A1 Diagram of the paired total soil and root exclusion collars used to partition the heterotrophic and autotrophic components of soil respiration. Created with BioRender.com

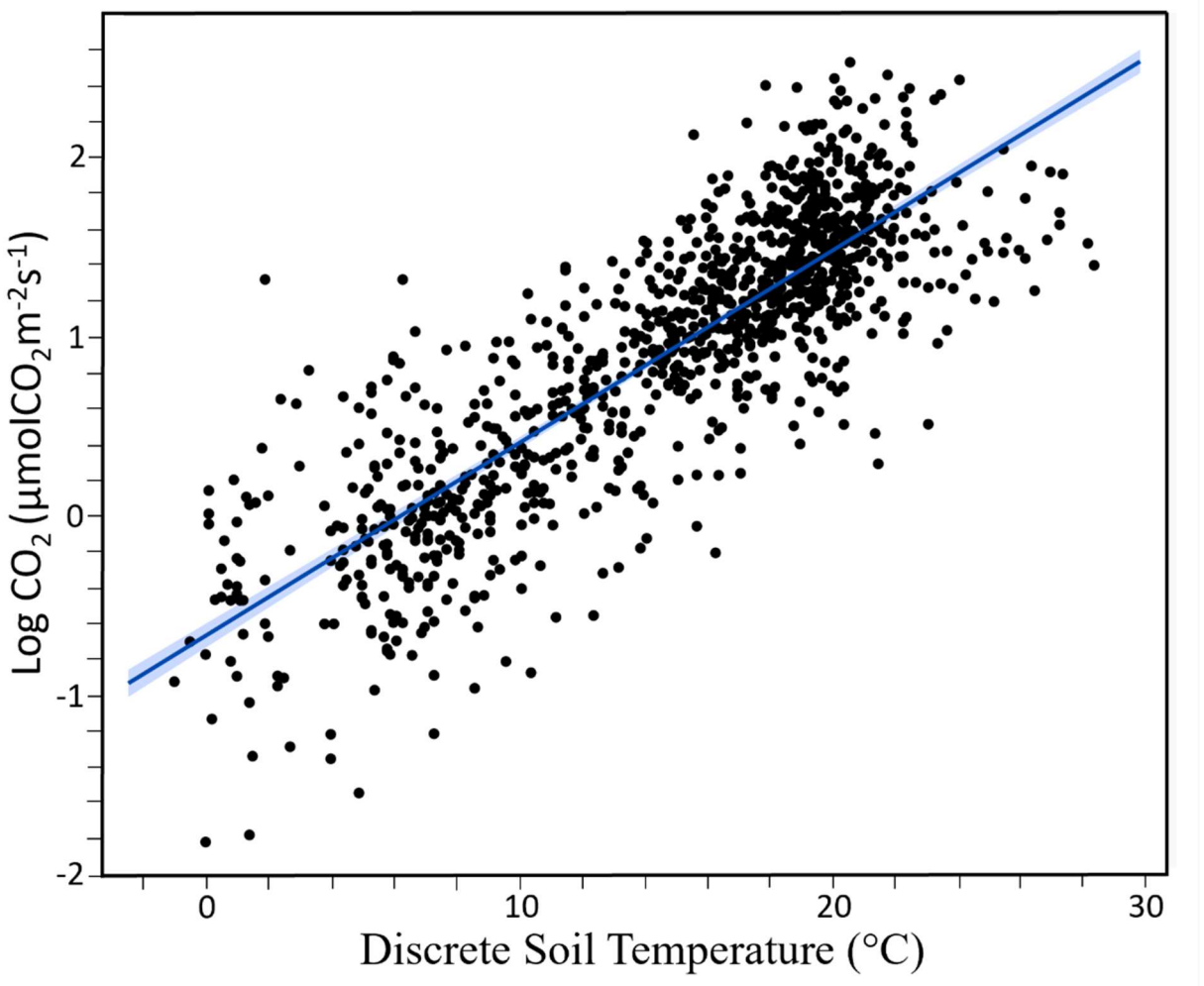

Figure A2 Linear regression between discrete soil temperature and CO_2 flux measured during 19 sampling trips between Jan 2021 and Dec 2022. Each collar location was fit individually for temperature modeling. Average collar-level $r^2 = 0.88$ (ranging from 0.66 to 0.99).

Table A1 List of each CO_2 flux collar and associated ID, plot ID, within-plot location, and whether it was included in the respiration partitioning study.

Collar ID	Plot ID	Collar location	Partitioned?
C2C1	Control 2	1	✓
C2C2	Control 2	2	✓
C2C3	Control 2	3	✓
C6C1	Control 6	1	✓
C6C2	Control 6	2	✓
C6C3	Control 6	3	✓
C9C1	Control 9	1	✓
C9C2	Control 9	2	✓
C9C3	Control 9	3	✓
G2C1	Gap 2	1	✓
G2C2	Gap 2	2	✓
G2C3	Gap 2	3	✓
G2C4	Gap 2	4	✓
G2C5	Gap 2	5	✓
G3C1	Gap 3	1	–
G3C2	Gap 3	2	–
G3C3	Gap 3	3	–
G3C4	Gap 3	4	–
G3C5	Gap 3	5	–
G7C1	Gap 7	1	✓
G7C2	Gap 7	2	✓
G7C3	Gap 7	3	✓
G7C4	Gap 7	4	✓
G7C5	Gap 7	5	✓
G11C1	Gap 11	1	–
G11C2	Gap 11	2	–
G11C3	Gap 11	3	–
G11C4	Gap 11	4	–
G11C5	Gap 11	5	–
G18C1	Gap 18	1	✓
G18C2	Gap 18	2	✓
G18C3	Gap 18	3	✓
G18C4	Gap 18	4	✓
G18C5	Gap 18	5	✓
G35C1	Gap 35	1	–
G35C2	Gap 35	2	–
G35C3	Gap 35	3	–
G35C4	Gap 35	4	–
G35C5	Gap 35	5	–
G36C1	Gap 36	1	–
G36C2	Gap 36	2	–
G36C3	Gap 36	3	–
G36C4	Gap 36	4	–
G36C5	Gap 36	5	–
G44C1	Gap 44	1	✓
G44C2	Gap 44	2	–
G44C3	Gap 44	3	✓
G44C4	Gap 44	4	✓
G44C5	Gap 44	5	✓
G54C1	Gap 54	1	✓
G54C2	Gap 54	2	✓
G54C3	Gap 54	3	✓
G54C4	Gap 54	4	✓
G54C5	Gap 54	5	✓
G57C1	Gap 57	1	–
G57C2	Gap 57	2	–
G57C3	Gap 57	3	–
G57C4	Gap 57	4	–
G57C5	Gap 57	5	–
G63C1	Gap 63	1	✓
G63C2	Gap 63	2	✓
G63C3	Gap 63	3	✓
G63C4	Gap 63	4	✓
G63C5	Gap 63	5	✓

Table A2 Temperature sensitivity (Q10) and linear r^2 values for each total soil CO_2 flux (non-exclusion collars) and root exclusion collar in the respiration partitioning study as well as the distance between the two collars. Q10 and r^2 values obtained from linear models of discrete CO_2 flux and T_S measurements.

	Non-Exclusion Collars		Root Exclusion Collars		
Collar ID	Q10	R_S by T_S linear r^2	Q10	R_S by T_S linear r^2	Distance between collars (m)
C2C1	5.625	0.89	3.842	0.91	0.635
C2C2	4.322	0.92	2.908	0.83	2.1844
C2C3	3.586	0.91	3.85	0.93	1.1938
C6C1	3.823	0.96	2.714	0.95	0.7493
C6C2	2.747	0.98	2.676	0.97	0.4064
C6C3	3.085	0.98	2.203	0.84	0.2032
C9C1	3.12	0.81	2.234	0.68	0.2794
C9C2	2.831	0.99	2.543	0.79	0.508
C9C3	3.031	0.90	2.327	0.92	0.2921
G18C1	3.929	0.95	2.502	0.89	0.5207
G18C2	3.351	0.93	2.717	0.88	2.7051
G18C3	3.092	0.98	2.415	0.96	1.0668
G18C4	3.711	0.97	2.763	0.96	1.2319
G18C5	3.048	0.85	2.544	0.95	1.4605
G2C1	3.991	0.93	3.828	0.94	0.6858
G2C2	4.972	0.96	3.415	0.97	0.37465
G2C3	3.775	0.86	3.029	0.63	0.3937
G2C4	3.022	0.96	2.749	0.93	0.889
G2C5	3.266	0.95	3.562	0.88	0.73025
G44C1	3.115	0.95	3.423	0.85	0.2667
G44C3	2.553	0.77	2.429	0.93	1.4097
G44C4	2.412	0.90	2.521	0.97	1.2192
G44C5	8.005	0.99	5.936	0.87	1.9939
G54C1	2.787	0.97	2.377	0.93	0.47625
G54C2	2.895	0.98	2.465	0.91	0.88265
G54C3	2.094	0.81	2.967	0.97	1.42875
G54C4	3.776	0.94	2.236	0.98	0.6985
G54C5	3.175	0.95	2.478	0.93	1.9304
G63C1	2.999	0.99	3.306	0.94	0.32385
G63C2	2.215	0.92	2.445	0.94	1.42875
G63C3	3.146	0.90	1.77	0.91	0.4445
G63C4	1.786	0.68	2.382	0.71	0.45085
G63C5	4.323	0.91	2.457	0.92	2.3114
G7C1	2.956	0.81	4.749	0.93	0.8382
G7C2	3.075	0.96	1.943	0.83	1.2573
G7C3	4.011	0.98	3.376	0.86	0.70485
G7C4	4.196	0.96	2.415	0.97	0.9017
G7C5	3.903	0.96	3.108	0.97	-

Table A3 Discrete (raw flux) and temperature modeled (RT_S flux) CO_2 flux from each measurement date for each total soil CO_2 flux collar (non-exclusion collars) in the control plots.

Collar ID		June 21-22	July 5-6	July 18-19	Aug 2	Aug 15-16	Sept 20-21	Oct 10-11	Nov 19 / Dec 2
C2C1	Raw flux	-	3.83504	7.26489	6.56522	6.68925	3.35252	1.76920	0.99783
	RT_S flux	-	5.20504	5.48184	5.67451	5.38798	4.53332	2.08390	0.87868
C2C2	Raw flux	5.50966	4.46132	3.70843	3.48434	3.39071	2.70396	1.42006	0.63525
	RT_S flux	3.50141	4.17377	3.87921	3.93641	3.76729	3.25430	1.58839	0.60448
C2C3	Raw flux	3.48758	4.75087	5.02047	4.16757	4.15606	3.00535	1.55773	0.97998
	RT_S flux	3.50566	4.30033	4.03434	4.13871	4.03434	3.64256	2.10347	0.84954
C6C1	Raw flux	3.19306	4.97196	-	5.17825	4.90055	3.03348	1.24140	0.75814
	RT_S flux	3.74718	5.10106	-	4.70668	3.90101	3.32114	1.44607	0.68239
C6C2	Raw flux	8.75691	8.61553	-	8.46785	8.82425	6.92366	3.56171	2.13115
	RT_S flux	7.86632	9.06172	-	8.97062	8.02692	7.25544	3.87771	2.05163
C6C3	Raw flux	3.56170	4.93519	-	4.56885	4.02671	2.91854	1.53247	0.98689
	RT_S flux	3.47396	4.76250	-	4.55263	3.71693	3.28366	1.68911	0.91923
C9C1	Raw flux	4.95117	6.13817	3.41988	5.59332	4.24462	4.27428	2.13134	-
	RT_S flux	4.19169	5.38399	4.64369	5.44560	4.48785	4.14426	2.11784	-
C9C2	Raw flux	5.19010	5.97661	4.80771	6.01075	4.62325	4.35914	2.30246	-
	RT_S flux	5.01815	6.17941	4.76369	5.80532	4.76369	4.42896	2.29897	-
C9C3	Raw flux	5.44768	6.23082	4.26474	4.85805	5.17461	4.27249	2.25182	-
	RT_S flux	4.82583	5.69916	4.87964	5.57415	4.77261	4.31929	2.27032	-

Table A4 Discrete (raw flux) and temperature modeled (RT_S flux) CO_2 flux from each measurement date for each total soil CO_2 flux collar (non-exclusion collars) in the large gap treatment plots.

Collar ID		June 21-22	July 5-6	July 18-19	Aug 2	Aug 15-16	Sept 20-21	Oct 10-11	Nov 19 / Dec 2
G2C1	Raw flux	5.29871	6.77782	8.22963	10.8453	9.69819	7.03774	3.89384	1.45908
	RT_S flux	6.59042	8.93624	8.11106	9.31511	8.22411	6.23547	3.63446	1.49878
G2C2	Raw flux	4.25104	4.97551	4.81825	6.10424	5.28659	3.72229	1.78342	0.63112
	RT_S flux	4.38441	4.67492	4.82731	5.23038	4.90536	3.79508	2.54144	0.56274
G2C3	Raw flux	-	-	5.96950	6.36774	5.33024	3.94050	2.17504	1.18568
	RT_S flux	-	-	5.02698	5.30131	4.89519	4.28627	3.51193	1.04850
G2C4	Raw flux	4.17848	4.65990	4.04260	5.42712	4.75703	3.11370	1.92082	0.91294
	RT_S flux	4.65306	4.40276	4.81002	5.19716	3.94183	2.82888	2.12199	0.91566
G2C5	Raw flux	4.70442	5.26584	6.42573	5.87368	5.84413	4.00853	2.25101	1.05472
	RT_S flux	5.15501	6.53185	5.40494	6.22981	4.85878	3.61425	2.38840	1.09356
G7C1	Raw flux	2.35289	4.30255	-	4.47757	4.72705	5.14608	1.94417	0.99993
	RT_S flux	3.85617	4.29760	-	4.39178	4.20545	3.46008	2.01249	1.00574
G7C2	Raw flux	2.86336	4.29121	-	4.64125	4.15856	2.74117	1.78909	1.10075
	RT_S flux	3.24707	4.11079	-	4.01948	3.93020	3.13948	1.89390	1.02112
G7C3	Raw flux	5.50821	7.18096	-	-	8.86752	5.45642	2.79724	1.47876
	RT_S flux	5.29850	6.99516	-	-	8.14990	5.83954	3.30413	1.35829
G7C4	Raw flux	5.88525	6.14941	-	8.02645	7.02587	6.11585	2.28097	1.15743
	RT_S flux	5.49189	7.00803	-	7.10925	7.42177	5.26063	2.88049	1.07088
G7C5	Raw flux	7.15633	6.25551	-	6.35094	6.67877	5.91162	3.10484	1.25665
	RT_S flux	5.61349	6.88550	-	7.17260	7.07559	5.24403	3.30069	1.28994
G18C1	Raw flux	5.95736	5.74700	5.87914	6.46775	7.07187	4.22863	2.39221	1.17795
	RT_S flux	4.91679	6.37661	6.03698	6.46446	5.87401	5.19340	2.54941	1.15285
G18C2	Raw flux	4.11560	5.65753	4.37569	4.03213	4.06262	3.07625	1.64162	0.86533
	RT_S flux	3.61155	4.48967	4.12531	4.27769	4.22628	3.74496	2.07082	0.77768
G18C3	Raw flux	4.78909	5.26870	5.57256	4.74761	5.73107	5.23899	2.69205	1.24348
	RT_S flux	4.57440	5.54223	5.17925	5.48002	5.35767	4.89499	2.91215	1.22091
G18C4	Raw flux	8.78192	7.21359	8.88694	8.20859	7.83503	6.01075	3.53013	1.30591
	RT_S flux	7.11191	8.21555	7.89860	8.21555	8.00287	7.11191	3.54916	1.30999
G18C5	Raw flux	-	7.48248	8.59020	7.19231	8.88860	8.95269	2.53120	2.05046
	RT_S flux	-	8.51208	7.87328	8.23220	7.87328	6.51441	3.81552	1.76844

Table A5 Discrete (raw flux) and temperature modeled (RT_S flux) CO_2 flux from each measurement date for each total soil CO_2 flux collar (non-exclusion collars) in the small gap treatment plots.

Collar ID		June 21-22	July 5-6	July 18-19	Aug 2	Aug 15-16	Sept 20-21	Oct 10-11	Nov 19 / Dec 2
G44C1	Raw flux	5.26712	5.54861	4.04436	5.25807	5.27943	4.73721	1.97354	1.18355
	RT_S flux	4.15054	6.10752	4.54546	5.70506	4.54546	4.81114	2.09922	1.20305
G44C3	Raw flux	6.80672	3.30691	7.18176	7.03556	5.98801	4.66988	4.12971	1.52226
	RT_S flux	6.39860	5.15787	5.45622	7.43374	5.40532	5.20644	2.91199	1.82255
G44C4	Raw flux	3.17329	-	1.99794	3.30029	2.05073	2.06458	1.38910	0.74041
	RT_S flux	2.47502	-	2.22683	3.45864	2.26640	2.18796	1.12044	0.86031
G44C5	Raw flux	-	7.04636	5.62232	9.50565	6.36629	5.76659	1.14777	0.64068
	RT_S flux	-	7.14142	6.04666	9.55554	6.04666	5.11973	1.38079	0.57639
G54C1	Raw flux	5.64286	7.54642	-	5.83159	6.83816	6.12967	3.25086	1.33454
	RT_S flux	5.80155	7.34417	-	6.97722	6.76591	5.34475	2.88936	1.45382
G54C2	Raw flux	10.1186	10.1894	-	10.3337	11.6983	8.63099	4.57519	2.33821
	RT_S flux	9.44804	10.9642	-	10.9642	10.5077	8.40538	5.09997	2.24944
G54C3	Raw flux	3.48550	5.41713	-	6.22720	7.46759	5.95651	3.21433	1.94596
	RT_S flux	5.00110	6.28875	-	5.92772	5.75505	4.89144	3.23368	1.92763
G54C4	Raw flux	6.02271	5.22847	-	5.02281	5.24243	5.19762	2.42971	0.90357
	RT_S flux	4.95374	6.04620	-	5.96640	5.58294	4.33745	2.11670	1.03296
G54C5	Raw flux	3.99763	4.61107	-	4.34773	4.96429	3.87868	2.37276	0.86910
	RT_S flux	4.21105	4.78168	-	5.00784	4.61880	3.58218	1.85421	1.02867
G63C1	Raw flux	-	5.89709	6.46614	6.16518	5.84089	5.16404	3.27003	1.32144
	RT_S flux	-	6.35432	5.94909	6.28491	5.94909	5.10123	3.14636	1.35065
G63C2	Raw flux	5.61306	6.31778	5.84672	-	6.49989	4.74928	3.07202	2.38268
	RT_S flux	5.25442	6.16018	5.82665	-	5.87317	5.25442	3.70317	2.17367
G63C3	Raw flux	5.30078	4.80625	4.18891	3.74446	3.36629	3.93507	1.96361	0.97174
	RT_S flux	3.68015	4.57539	4.22269	4.22269	4.17458	3.68015	2.32695	0.94104
G63C4	Raw flux	3.88742	-	4.28221	-	3.42923	4.64266	1.91901	1.94251
	RT_S flux	3.56794	-	3.93750	-	4.00659	3.67288	2.78067	1.71856
G63C5	Raw flux	7.00940	7.58802	4.81054	5.70465	6.78337	6.23809	2.32214	1.13522
	RT_S flux	5.21700	6.78977	6.40361	6.78977	6.40361	5.29393	2.86263	1.08937

Table A6 Discrete (raw flux) and temperature modeled (RT_S flux) CO_2 flux from each measurement date for each root exclusion collar in the control plots.

Collar ID		June 21-22	July 5-6	July 18-19	Aug 2	Aug 15-16	Sept 20-21	Oct 10-11	Nov 19 / Dec 2
C2C1 Excl.	Raw flux	3.95544	4.85646	4.69179	5.94721	4.91967	2.85247	1.76729	1.12722
	RT_S flux	3.76725	4.54841	4.54841	4.86504	4.61004	4.02950	2.14052	0.99388
C2C2 Excl.	Raw flux	5.67580	6.44604	5.00963	5.23298	5.11448	4.16319	2.03714	1.90645
	RT_S flux	4.47962	5.37087	5.20161	5.48675	5.20161	4.72518	2.89191	1.62506
C2C3 Excl.	Raw flux	4.13171	6.80280	7.66878	5.88817	4.79920	5.55574	2.64362	1.23272
	RT_S flux	4.95959	5.98980	5.75239	5.90960	5.75239	5.83046	2.74055	1.18808
C6C1 Excl.	Raw flux	2.39374	3.45702	4.33550	3.72607	3.78932	2.41780	1.39714	0.85526
	RT_S flux	2.95450	3.71733	3.68039	3.50114	3.26477	2.70055	1.46861	0.79866
C6C2 Excl.	Raw flux	4.11305	5.61316	5.59510	6.01956	5.65792	5.15047	2.65326	1.40925
	RT_S flux	4.89501	5.29611	5.96023	5.73008	5.24423	4.89501	2.65873	1.40207
C6C3 Excl.	Raw flux	4.13453	5.09653	4.60145	3.48966	3.30587	2.42117	1.98134	1.40654
	RT_S flux	3.37648	4.21231	4.11366	4.08129	3.54036	3.29741	2.03662	1.32941
C9C1 Excl.	Raw flux	4.85198	5.05043	3.14439	4.49364	4.29374	4.33148	2.36033	-
	RT_S flux	3.93018	4.69019	4.22495	4.72803	4.12431	4.12431	2.42672	-
C9C2 Excl.	Raw flux	6.10470	6.44599	4.00656	4.92580	3.82014	4.30332	2.43539	-
	RT_S flux	4.71683	5.68465	4.50181	5.37511	4.50181	4.54401	2.34261	-
C9C3 Excl.	Raw flux	6.86904	7.16281	6.14713	6.17252	6.58879	5.59546	3.44264	-
	RT_S flux	6.22316	7.06383	6.27595	6.94549	6.22316	5.67096	3.50385	-

Table A7 Discrete (raw flux) and temperature modeled (RT_S flux) CO_2 flux from each measurement date for each root exclusion collar in the large gap treatment plots.

Collar ID		June 21-22	July 5-6	July 18-19	Aug 2	Aug 15-16	Sept 20-21	Oct 10-11	Nov 19 / Dec 2
G2C1 Excl.	Raw flux	4.31324	4.92292	4.33414	4.95812	4.36305	2.86349	1.61811	0.91592
	RT_S flux	3.51753	4.47901	4.30221	4.92033	4.41929	3.28917	2.14051	0.81421
G2C2 Excl.	Raw flux	4.37626	5.50458	5.10432	4.89758	5.24175	3.78548	2.36168	1.01777
	RT_S flux	4.52843	4.75644	4.87471	5.18343	4.81521	4.00509	2.87479	0.95189
G2C3 Excl.	Raw flux	3.67287	4.93478	9.09370	7.29078	5.29990	4.24264	2.62976	1.67741
	RT_S flux	4.01648	5.24044	5.18268	5.85467	5.47800	4.53725	4.84924	1.54842
G2C4 Excl.	Raw flux	7.86984	8.08420	6.94090	8.94335	7.25224	4.28283	2.92570	1.69911
	RT_S flux	7.76292	7.01633	6.73820	8.41700	7.15967	4.49658	4.14715	1.47847
G2C5 Excl.	Raw flux	5.54623	6.11625	5.77656	5.35760	4.17347	3.81738	1.18351	1.00486
	RT_S flux	6.14295	5.01300	5.54929	5.54929	4.19617	2.94012	2.03403	0.83587
G7C1 Excl.	Raw flux	3.02847	2.94355	-	4.71855	2.81093	1.92921	1.38643	0.43468
	RT_S flux	2.62149	3.36360	-	3.47006	3.36360	2.46311	1.16603	0.46506
G7C2 Excl.	Raw flux	3.45058	5.04991	4.40894	4.38301	4.49548	3.17614	2.33641	2.34636
	RT_S flux	3.81466	4.24233	4.32770	4.35654	4.21425	3.66564	2.73679	2.04330
G7C3 Excl.	Raw flux	5.42732	6.14784	6.25902	7.74876	6.41538	4.94756	1.86640	1.79394
	RT_S flux	4.81766	5.99722	6.69125	6.37339	6.45141	4.99676	2.99748	1.44447
G7C4 Excl.	Raw flux	4.85818	4.27582	4.88468	5.00675	4.76104	3.34504	2.37565	1.42000
	RT_S flux	4.34302	4.53877	5.18055	4.74334	4.53877	3.48387	2.62741	1.35625
G7C5 Excl.	Raw flux	4.85818	4.27582	4.88468	5.00675	4.76104	3.34504	2.37565	1.42000
	RT_S flux	5.69824	6.75495	6.75495	7.14907	6.90992	5.50763	3.38198	1.71256
G18C1 Excl.	Raw flux	5.65513	6.28711	7.68058	9.00451	8.14814	5.03170	3.66243	2.51056
	RT_S flux	6.07041	7.49572	7.22576	7.29232	6.96553	6.01500	3.94498	2.33909
G18C2 Excl.	Raw flux	6.58700	7.60210	5.82734	6.22693	5.98153	4.80720	2.72040	2.02077
	RT_S flux	5.37063	6.36527	6.11581	6.23929	6.11581	5.64584	3.52953	1.80672
G18C3 Excl.	Raw flux	4.86143	6.73510	6.55849	6.64847	7.09488	6.43812	3.69197	2.09361
	RT_S flux	5.61900	6.52741	6.47012	6.47012	6.35705	6.24596	4.20072	1.96828
G18C4 Excl.	Raw flux	6.49064	9.38260	7.71033	7.67338	8.05557	7.23842	3.82904	1.98025
	RT_S flux	7.20246	7.50127	8.05434	7.89229	7.89229	7.35035	4.20301	1.90239
G18C5 Excl.	Raw flux	3.11024	4.83022	4.18931	4.51658	4.48887	3.92312	1.98137	1.17237
	RT_S flux	3.86146	4.40068	4.27913	4.27913	4.19996	3.58355	2.26791	1.09483

Table A8 Discrete (raw flux) and temperature modeled (RT_S flux) CO_2 flux from each measurement date for each root exclusion collar in the small gap treatment plots.

Collar ID		June 21-22	July 5-6	July 18-19	Aug 2	Aug 15-16	Sept 20-21	Oct 10-11	Nov 19 / Dec 2
G44C1 Excl.	Raw flux	3.75634	5.34809	4.94983	3.53844	3.59883	6.23953	1.88620	0.84869
	RT_S flux	3.71138	5.63954	4.09535	5.23815	4.19739	3.89864	1.77368	0.97051
G44C3 Excl.	Raw flux	5.69952	5.05651	4.84436	5.77952	5.13305	4.70294	3.45475	1.61137
	RT_S flux	4.95903	4.87179	4.95903	6.76531	5.04783	4.87179	2.99032	1.81925
G44C4 Excl.	Raw flux	6.24347	6.27481	4.44295	7.90133	4.55508	4.55407	2.77381	1.76946
	RT_S flux	6.14241	5.39661	5.01183	7.59795	5.10537	4.65449	2.62366	1.77932
G44C5 Excl.	Raw flux	6.17397	5.15933	4.82470	5.09611	5.24798	4.49322	1.98403	0.49885
	RT_S flux	3.77760	5.58957	5.11334	7.98125	4.93441	3.91458	1.57841	0.69571
G54C1 Excl.	Raw flux	9.81718	11.3067	9.49486	9.00962	8.49847	9.49404	4.12902	2.74989
	RT_S flux	8.50118	10.3744	10.1963	9.93493	9.68019	7.86387	4.84238	2.64142
G54C2 Excl.	Raw flux	10.0611	10.7139	9.21783	10.9445	9.83738	11.1591	6.57703	2.44995
	RT_S flux	9.52950	10.8122	11.7265	10.8122	10.7151	8.78645	5.54657	2.81980
G54C3 Excl.	Raw flux	3.83177	4.55547	6.27207	5.06984	5.27745	-	2.05167	1.06380
	RT_S flux	4.33292	5.04543	5.15637	5.10060	5.10060	-	2.11389	1.03130
G54C4 Excl.	Raw flux	4.34873	4.03480	4.23545	4.13474	4.22053	3.39210	1.94243	1.47239
	RT_S flux	3.82642	4.28267	4.21431	4.24835	4.18053	3.44639	2.10962	1.41085
G54C5 Excl.	Raw flux	11.8709	9.47808	9.24720	9.06898	8.92845	6.90545	4.18212	3.09221
	RT_S flux	9.05885	9.65285	9.14142	10.0096	9.30881	7.55557	4.58723	2.91431
G63C1 Excl.	Raw flux	7.96871	7.47429	8.97004	7.16807	6.64815	5.49295	4.10384	1.36531
	RT_S flux	6.28670	8.08104	7.52163	7.98500	7.61210	6.28670	3.67075	1.46192
G63C2 Excl.	Raw flux	5.03554	6.44484	5.49742	-	6.02244	4.35209	2.86424	1.84918
	RT_S flux	4.83969	5.68452	5.53411	-	5.58380	5.10634	3.32486	1.71595
G63C3 Excl.	Raw flux	3.46459	3.42112	4.17849	3.30025	3.12532	3.10893	2.48997	1.52675
	RT_S flux	3.22520	3.59471	3.45389	3.45389	3.43423	3.22520	2.61109	1.50941
G63C4 Excl.	Raw flux	4.81857	7.16252	5.43406	2.99367	3.63289	4.09934	2.79121	1.45011
	RT_S flux	3.99502	4.75228	4.55047	4.59013	4.59013	4.20857	3.13317	1.41002
G63C5 Excl.	Raw flux	5.58102	6.20374	5.39373	4.87591	4.56411	3.92522	2.86481	1.59674
	RT_S flux	4.49309	5.47575	5.23506	5.28233	5.18820	4.57461	2.89218	1.59783